Optical sum rule violation, superfluid weight and condensation energy in the cuprates

J. E. Hirsch[a] and F. Marsiglio[b]

[a]*Department of Physics, University of California, San Diego, La Jolla, CA 92093-0319*
[b]*Department of Physics, University of Alberta, Edmonton, Alberta, Canada T6G 2J1*

(February 1, 2008)

The model of hole superconductivity predicts that the superfluid weight in the zero-frequency δ-function in the optical conductivity has an anomalous contribution from high frequencies, due to lowering of the system's kinetic energy upon entering the superconducting state. The lowering of kinetic energy, mainly in-plane in origin, accounts for both the condensation energy of the superconductor as well as an increased potential energy due to larger Coulomb repulsion in the paired state. It leads to an apparent violation of the conductivity sum rule, which in the clean limit we predict to be substantially larger for in-plane than for c-axis conductivity. However, because cuprates are in the dirty limit for c-axis transport, the sum rule violation is found to be greatly enhanced in the c-direction. The model predicts the sum rule violation to be largest in the underdoped regime and to decrease with doping, more rapidly in the c-direction that in the plane. So far, experiments have detected sum rule violation in c-axis transport in several cuprates, as well as a decrease and disappearance of this violation for increasing doping, but no violation in-plane. We explore the predictions of the model for a wide range of parameters, both in the absence and in the presence of disorder, and the relation with current experimental knowledge.

I. INTRODUCTION

In the model of hole superconductivity the hopping amplitude for a hole of spin σ hopping between sites i and j is given by [1,2]

$$t_{ij}^\sigma = t_{ij}^h + (\Delta t)_{ij}(n_{i,-\sigma} + n_{j,-\sigma}) \tag{1}$$

with $n_{i,-\sigma}$ the occupation number for spin $(-\sigma)$ at site i. Eq. (1) leads to superconductivity at low hole concentration due to lowering of the carrier's effective mass, or equivalently of kinetic energy, upon pairing. In tight binding models for low carrier concentration the hopping amplitude is related to the effective mass m^* through

$$t = \frac{\hbar^2}{2m^*a^2} \tag{2}$$

with a the lattice spacing in the given direction.

This physics leads to nontrivial consequences for the electrodynamics of hole superconductors [3,4]. The London penetration depth in the limit of low carrier concentration is given by

$$\lambda = \left(\frac{m^*c^2}{4\pi n_s e^{*2}}\right)^{1/2} \tag{3}$$

with m^*, e^* the mass and charge of the superfluid carriers, and n_s the superfluid density. If the effective mass decreases upon pairing, λ will be smaller than expected from the normal state effective mass [3]. This leads to a violation [4] of the low energy optical sum rule (Ferrell-Glover-Tinkham sum rule [5]) which relates the London penetration depth (which depends on the effective mass in the paired state) to the low frequency 'missing area' in the optical conductivity (which is a function of the effective mass in the normal state). Observation of such a violation in several cuprates [6], long after it was predicted theoretically [4], lends support to the model upon which the prediction was based. The London penetration depth is determined by the weight of the zero-frequency δ-function in the optical conductivity ('superfluid weight'), which is predicted to be larger than the area missing from the low frequency optical absorption, as shown schematically in Fig. 1.

The sum rule violation is a manifestation of the lowering of kinetic energy that occurs upon pairing, and this lowering of kinetic energy is what gives the condensation energy of the superconductor within our model. In fact, the kinetic energy lowering (mainly from in-plane motion) that we obtain is much larger than the condensation energy [7], but is compensated to some extent by increase of Coulomb repulsion between carriers, that are on the average closer to each other in the paired state compared to the situation in the unpaired state.

Anderson [8] has proposed a mechanism for high T_c superconductivity based on lowering of kinetic energy of pairs tunneling between planes (interlayer tunneling theory, or ILT). That theory has in common with the one discussed here that superconductivity is driven by kinetic energy lowering, but it differs in that it only deals with c-axis transport. There are also other fundamental differences with the theory discussed here. According to ILT, the weight in the $\delta-$function for c-axis transport should account for the condensation energy of the superconductor, and it is claimed [8] that this is in fact the case in $La_{2-x}Sr_xCuO_4$ throughout the entire doping regime, from underdoped to overdoped. This implies in particular that within ILT theory the entire weight in the δ-function reflects lowering of c-axis kinetic energy, irrespective of whether that weight comes from low or from high frequency optical response. Thus, while the theory may be *consistent* with the observed c-axis sum rule violation [9], it makes no definite *prediction* on whether sum rule violation in the c direction should occur in a given doping regime. Or, perhaps one should interpret the ILT prediction to mean that the sum rule violation should be 100% for any doping regime, which however is inconsistent with reported observations [6]. Instead, our theory associates with kinetic energy lowering only the part of the $\delta-$function that comes from high frequencies, and yields quantitative predictions for it as well as for the total superfluid weight as a function of doping, which we will compare here with experiment.

Furthermore, for $Tl_2Ba_2CuO_y$ ILT theory cannot account for the condensation energy even using the entire weight in the zero-frequency δ-function, because it is too small by at least two orders of magnitude [10]. This is because ILT theory only considers kinetic energy lowering due to c-axis motion. Instead, the theory considered here, despite using only the fraction of the δ-function weight coming from high frequencies, has no trouble accounting for the condensation energy seen experimentally because it considers both c-axis as well as in-plane kinetic energy lowering.

In the anisotropic structure of the oxides the sum rule violation will naturally not be the same in all directions. We assume as the simplest possible model, that the ratio of t and Δt in Eq. (1) is the same in all directions. We will show that under this plausible assumption our model predicts the in-plane violation to be several times larger than the c-axis violation. This is in apparent contradiction with the reported experimental observation [6] of large c-axis sum rule violation ($\sim 50\%$) and no detectable in-plane violation($< 10\%$).However, a natural explanation for this discrepancy arises from the fact that the cuprates quite generally appear to be in the clean limit for in-plane conduction and in the dirty limit for c-axis conduction. We will not go here into a discussion of why this is the case, but there seems to be ample experimental evidence for it [11–14]. We show that under those conditions the c-axis violation is very greatly enhanced and will generally be much larger than the in-plane violation, in agreement with observations. The effect of disorder on the sum rule violation is schematically shown in Fig. 1.

Concerning the doping dependence, it is important to differentiate between relative and absolute values of kinetic energy lowering. For absolute values, our model predicts that the kinetic energy lowering is maximum close to the optimally doped case, and decreases smoothly both for underdoped and overdoped regimes. Instead, for the degree of sum rule violation, i.e. kinetic energy lowering relative to total superfluid weight, the model predicts a monotonic decrease as the doping increases (except in extremely underdoped regimes). Furthermore in the presence of disorder the rate of decrease with doping can be greatly enhanced. Experimentally, a rapid decrease of sum rule violation with doping has been observed [6], and we will show that the theory is compatible with the reported observations within reasonable assumptions.

Because of the difficulty in precisely estimating the appropiate parameters in our model for given materials, we explore here predictions of the model for a range of interaction parameters. This is of intrinsic interest, and furthermore it may be relevant to materials as yet undiscovered. Some general trends found are that for given maximum T_c the model predicts increasing sum rule violation as the nearest neighbor repulsion increases, and as the bandwidth decreases. The latter in turn also leads to an increasing condensation energy. The results that we obtain are compatible with existing observations in the cuprates for a range of parameters in the model, and future more accurate observations should be able to determine more precisely the parameters in the model to represent the physics of a given cuprate.

In Sect. II we review the Hamiltonian and general formalism, and discuss the calculation of the condensation energy. Sect. III discusses the optical sum rule predictions, in the clean limit, and in the presence of disorder. Sect. IV shows results for the clean limit for the full 3-dimensional anisotropic model for a variety of parameters, and in sect. V we compare the predictions of the model with experimental results taking into account the effect of disorder. We conclude in Sect. VI with a summary and discussion.

II. FORMALISM

The model is defined by the single band Hamiltonian [1]

$$H = -\sum_{i,j,\sigma} t_{ij}^{\sigma}(c_{i\sigma}^{\dagger} c_{j\sigma} + h.c.) + U \sum_{i} n_{i\uparrow} n_{i\downarrow} + \sum_{<ij>} V_{ij} n_i n_j \tag{4}$$

with i, j sites on a three-dimensional cubic lattice, and t_{ij}^σ defined by Eq. (1). $c_{i\sigma}^\dagger$ creates a hole of spin σ in the oxygen $p\pi$ planar orbital at site i, and other orbitals (Op_σ, $Cud_{x^2-y^2}$) are ignored [15]. We define t_{ij}^h in Eq. (1) to be t_a^h or t_c^h for nearest neighbor sites in the plane or in the c-direction, and similarly Δt_a, Δt_c, and assume the same anisotropy for t and Δt:

$$\eta = \frac{t_a}{t_c} = \frac{\Delta t_a}{\Delta t_c}. \tag{5}$$

The effective hopping as a function of hole density n_h is given by, with $\alpha = a$ or c:

$$t_\alpha = t_\alpha^h + \Delta t_\alpha n_h \tag{6}$$

and the effective mass anisotropy

$$\frac{m_c^*}{m_a^*} = \frac{t_a}{t_c} = \eta \tag{7}$$

is independent of doping level with this assumption. We assume isotropic nearest neighbor repulsion for simplicity; any anisotropy in it should be much smaller than that for the hopping amplitudes .

The formalism we use is described in Ref. [1]. The results are not very dependent on details of the band structure. To understand the behavior emerging from the planar motion, which dominates the energetics, one can use a simple constant density of states model,

$$g(\epsilon) = \frac{1}{D} \tag{8}$$

with D the bandwidth. This model illustrates well the behavior emerging from the planar motion [7]. Since we are interested in the anisotropy of various measured properties, we will mostly use here a three-dimensional tight-binding band structure, with a strong hopping anisotropy ($\eta = 25$, for definiteness). The consequences of this anisotropy for various properties have already been discussed in Refs. [1,3]. In particular, we discussed an approximation in which only energy integrations are required; anisotropy only enters through various weighted densities of states. The results thus obtained were very accurate.In the rest of this paper, unless stated otherwise, we will use this approximation [16].

The condensation energy per site is given by

$$\epsilon_{cond} = \epsilon_n - \epsilon_s \tag{9}$$

with ϵ_s, ϵ_n the average energy per site at the same temperature and for the same number of holes in the superconducting and normal states respectively. We define the different contributions

$$\epsilon_{cond} = \epsilon_t + \epsilon_{\Delta t} + \epsilon_U + \epsilon_V \tag{10}$$

arising from single particle hopping, correlated hopping, on-site and nearest neighbor repulsion respectively. All contributions to ϵ_{cond} in Eq. (10) except $\epsilon_{\Delta t}$ are negative: the single particle hopping energy is lowest in the normal state ($\epsilon_t < 0$), and the Coulomb repulsions due to U and V increase in the superconducting state ($\epsilon_U, \epsilon_V < 0$) because carriers in a pair are closer together on average. The condensation energy is entirely given by the large kinetic energy lowering due to correlated hopping ($\epsilon_{\Delta t}$) which is compensated to some extent by the other terms in Eq. (10). In weak coupling the condensation energy is given by the usual expression

$$\epsilon_{cond} = \frac{\Delta_0^2}{2} g(\epsilon_F) \tag{11}$$

with Δ_0 the energy gap and $g(\epsilon_F)$ the density of states at the Fermi energy.

To determine the various energies that contribute to the condensation energy, we define, as in previous work, the integrals

$$I_\ell = \int d\epsilon \left(-\frac{\epsilon}{D/2}\right)^\ell g(\epsilon) \frac{1 - 2f(E(\epsilon))}{2E(\epsilon)} \tag{12}$$

with f the Fermi function and the quasiparticle energy $E(\epsilon)$ given by

$$E(\epsilon) = \sqrt{(\epsilon - \mu)^2 + \Delta(\epsilon)^2} \tag{13a}$$

$$\Delta(\epsilon) = \Delta_m(-\frac{\epsilon}{D/2} + c) \tag{13b}$$

and the parameters Δ_m and c obtained from solution of the BCS equations. The various contributions to the condensation energy are given by

$$\epsilon_t = 2 \int d\epsilon \, g(\epsilon) \, \epsilon \, f(\epsilon - \mu_N) - D[\frac{D}{2}I_2 + \mu I_1] \tag{14a}$$

$$\epsilon_{\Delta t} = 2K\Delta_m^2(I_1 + cI_0)(I_2 + cI_1) \tag{14b}$$

$$\epsilon_U = -U\Delta_m^2(I_1 + cI_0)^2 \tag{14c}$$

$$\epsilon_V = -W\Delta_m^2(I_2 + cI_1)^2 \tag{14d}$$

with

$$K = 2z\Delta t \tag{15a}$$

$$W = zV \tag{15b}$$

and z the number of nearest neighbors to a site. Note that μ_N is the chemical potential required for n electrons in *the normal state*.

The contributions (14b,14c,14d) are useful in that they specify the various energy contributions arising from interaction terms in the Hamiltonian. They can, however, be summed, with the help of the gap equation [1], to give a single result

$$\epsilon_{\text{int}} \equiv \epsilon_{\Delta t} + \epsilon_U + \epsilon_V = \int d\epsilon \, g(\epsilon) \, \Delta^2(\epsilon) \frac{1 - 2f(E(\epsilon))}{2E(\epsilon)}, \tag{16}$$

in agreement with the usual expression for the internal energy contribution.

III. OPTICAL SUM RULE

The real part of the optical conductivity for light polarized in direction δ is given by [17]

$$\sigma_{1\delta}(\omega, T) = \frac{\pi}{\hbar\Omega Z} \sum_{n,m} \frac{e^{-\beta E_n} - e^{-\beta E_m}}{E_m - E_n} < n|J_\delta|m >< m|J_\delta|n > \delta(\omega - \frac{E_m - E_n}{\hbar}) \tag{17}$$

where n, m run over all eigenstates of the system with energies E_n, E_m, Z is the partition function, Ω the volume, and J_δ the component of the paramagnetic current operator in the δ direction. To derive the current operator for the tight binding model Eq. (4) we define the polarization operator

$$\vec{P} = e \sum_i \vec{R}_i n_i \tag{18}$$

and obtain the current operator from its time derivative

$$\vec{J} = \frac{d\vec{P}}{dt} = \frac{i}{\hbar}[H, \vec{P}] \tag{19}$$

yielding for the component in the δ direction

4

$$J_\delta = \frac{iea_\delta}{\hbar} \sum_{i,\sigma} t_{ij}^\sigma [c_{i+\delta,\sigma}^\dagger c_{i\sigma} - c_{i\sigma}^\dagger c_{i+\delta,\sigma}]. \tag{20}$$

Note that the hopping amplitudes in Eq. (20) have the operator dependence given by Eq. (1), but because density operators commute with each other the form Eq. (20) is the same as in the ordinary tight binding model with constant hopping amplitude. Similarly the commutator of the current and polarization operators yields

$$[J_\delta, P_\delta] = -\frac{ie^2}{\hbar} a_\delta^2 < -T_\delta > \tag{21}$$

where a_δ is the lattice spacing in the δ direction and T_δ is the part of the kinetic energy arising from hopping processes in the δ direction:

$$T_\delta = -\sum_i t_{i,i+\delta}^\sigma [c_{i\sigma}^\dagger c_{i+\delta,\sigma} + h.c.]. \tag{22}$$

Using Eq. (19) we can write

$$\frac{< n|J_\delta|m >< m|J_\delta|n >}{E_m - E_n} = \frac{i}{2\hbar}[< n|J_\delta|m >< m|P_\delta|n > - < n|P_\delta|m >< m|J_\delta|n >]. \tag{23}$$

Substituting in Eq. (17), integrating over frequency and summing over intermediate states yields the 'partial' conductivity sum rule for our model:

$$\int_0^{\omega_m} d\omega \sigma_{1\delta}(\omega, T) = \frac{\pi^2 a_\delta^2 e^2}{2\hbar^2 \Omega} < -T_\delta > \tag{24}$$

which formally looks the same as in the usual tight binding model [18]. The high frequency cutoff ω_m in Eq. (24) indicates that transitions to higher energy states not described by our Hamiltonian Eq. (4) are excluded. If we were to extend the integral to infinity instead, the usual conductivity sum rule follows:

$$\int_0^\infty d\omega \sigma_{1\delta}(\omega, T) = \frac{\pi e^2 n}{2m}, \tag{25}$$

where n is the electron density and m the bare electron mass. For the tight binding model with a nearly empty or a nearly full band it is easily seen that Eq. (24) takes the form Eq. (25) with m replaced by the effective mass m^* given by Eq. (2).

More generally, the complex frequency-dependent conductivity for light polarized in direction δ is given by [17]

$$\sigma_\delta(\omega) = \frac{i}{\omega}[\Pi_\delta(\omega) - \frac{e^2 a_\delta^2}{\hbar^2 \Omega} < T_\delta >] \tag{26}$$

with Π_δ the complex current-current correlation function, with spectral representation

$$\Pi_\delta(\omega) = \frac{1}{\Omega Z} \sum_{n,m} \frac{e^{-\beta E_n} - e^{-\beta E_m}}{E_m - E_n + \hbar\omega + i\delta} < n|J_\delta|m >< m|J_\delta|n > \tag{27}$$

and the London Kernel, that gives the penetration depth λ_δ, is given by

$$K_\delta = \frac{1}{\lambda_\delta^2} = \frac{4\pi\omega}{c^2} \sigma_{2\delta} \tag{28}$$

with σ_2 the imaginary part of the conductivity. Hence,

$$K_\delta = \frac{4\pi}{c^2} \Pi_{1\delta} - \frac{4\pi e^2 a_\delta^2}{c^2 \hbar^2 \Omega} < T_{1\delta} > \equiv K_{1\delta} + K_{2\delta} \tag{29}$$

with $\Pi_{1\delta}$ the real part of the current-current correlation function. $K_{1\delta}$ and $K_{2\delta}$ are the paramagnetic and diamagnetic London Kernels.

In the superconducting state at temperature T the real part of the conductivity is

$$\sigma_{1\delta}^s = D_\delta(T)\delta(\omega) + \sigma_{1\delta}^{s,reg}(\omega,T). \tag{30}$$

The superfluid weight, $D_\delta(T)$, gives rise, through a Kramers-Kronig relation, to a $1/\omega$ contribution to the imaginary part of the conductivity and hence to the London Kernel

$$K_\delta = \frac{8D_\delta}{c^2}. \tag{31}$$

Integrating Eq. (30) and using Eq. (24) yields

$$D_\delta(T) + \int_{0^+}^{\omega_m} \sigma_{1\delta}^s(\omega,T) = \frac{\pi e^2 a_\delta^2 e^2}{2\hbar^2 \Omega} < -T_\delta >_{s,T}. \tag{32}$$

On the other hand in the normal state at temperature T_1

$$\int_0^{\omega_m} \sigma_{1\delta}^n(\omega,T_1) = \frac{\pi e^2 a_\delta^2 e^2}{2\hbar^2 \Omega} < -T_\delta >_{n,T_1} \tag{33}$$

and Eqs. (32) and (33) yield

$$D_\delta(T) = \int_{0^+}^{\omega_m} d\omega [\sigma_{1\delta}^n(\omega,T_1) - \sigma_{1\delta}^s(\omega,T)] + \frac{\pi e^2 a_\delta^2}{2\hbar^2 \Omega}[< -T_\delta >_{s,T} - < -T_\delta >_{n,T_1}] \equiv \delta A_l + \delta A_h. \tag{34}$$

The first term in Eq. (34) is the 'low frequency missing area' δA_l that arises from the opening of the superconducting energy gap, as discussed by Ferrell, Glover and Tinkham. It is *not* related to *changes* in kinetic energy in going into the superconducting state, but reflects simply the kinetic energy of the carriers in the normal state. In conventional superconductors, only this term is expected to contribute to the superfluid weight. The second term in Eq. (34) was predicted to exist in high T_c materials in 1992 [4], and experimental evidence for its existence was found in 1999 [6]. The qualitative behavior of $\sigma_1(\omega)$ and the different contributions to the superfluid weight are shown schematically in Figure 1.

Integrating Eqs. (30) and (33) to infinity instead should yield the same answer according to the 'global' sum rule Eq. (25), so that we have also

$$D_\delta(T) = \int_{0^+}^{\infty} d\omega [\sigma_{1\delta}^n(\omega,T_1) - \sigma_{1\delta}^s(\omega,T)] = \delta A_l + \delta A_h \tag{35}$$

and

$$\delta A_h = \int_{\omega_m}^{\infty} d\omega [\sigma_{1\delta}^n(\omega,T_1) - \sigma_{1\delta}^s(\omega,T)] = \frac{\pi e^2 a_\delta^2}{2\hbar^2 \Omega}[< -T_\delta >_{s,T} - < -T_\delta >_{n,T_1}] \tag{36}$$

so that the change in optical absorption at high frequencies is given by the change in kinetic energy. The states involved in the optical transitions that contribute to Eq. (36) are *not* in the Hilbert space where the Hamiltonian Eq. (4) is defined. However, a more general Hamiltonian can be found [19] that both contains these states and yields Eq. (4) as a low energy effective Hamiltonian when these states are projected out.

Expressions for the kinetic energies are given in Refs. [3,4]; we reproduce them here for completeness:

$$< T_\delta > = < T_\delta^t > + < T_\delta^{\Delta t} > \tag{37a}$$

$$< T_\delta^t > = -2(t_\delta^h + n\Delta t_\delta) \sum_k cosk_\delta (1 - \frac{\epsilon_k - \mu}{E_k}(1 - 2f(E_k))) \tag{37b}$$

$$< T_\delta^{\Delta t} > = -\frac{4\Delta t_\delta}{N} \sum_{k,k'} (cosk_\delta + cosk'_\delta) \frac{\Delta_k}{2E_k} \frac{\Delta_{k'}}{2E_{k'}} (1 - 2f(E_k))(1 - 2f(E_{k'})). \tag{37c}$$

Eq. (36) shows that if there is a change in the carrier's kinetic energy in going from the normal state at temperature T_1 to the superconducting state at temperature T, there will be an apparent violation of the conductivity sum rule. Such a change arises in our model from the pair contribution to the kinetic energy, Eq. (37c), which is zero above T_c and becomes non-zero (negative) below T_c as the superconducting state develops.

The superfluid weight and missing areas are related to the London Kernel K_δ by

$$D_\delta = \delta A_l^\delta + \delta A_h^\delta = \frac{c^2}{8} K_\delta \tag{38}$$

$$K_\delta = K_{1\delta} + K_{2\delta}. \tag{39}$$

The diamagnetic part of the London Kernel K_2 is given by

$$K_{2\delta} = \frac{4\pi e^2 a_\delta^2}{\hbar^2 c^2 \Omega} [< -T_\delta^t > + < -T_\delta^{\Delta t} >]. \tag{40}$$

The low frequency missing area is given by the London paramagnetic Kernel and the single particle part of the kinetic energy

$$\delta A_l = \frac{c^2}{8} [K_{1\delta} + \frac{4\pi e^2 a_\delta^2}{\hbar^2 c^2 \Omega} < -T_\delta^t >], \tag{41}$$

and the high frequency missing area by the remaining part of the London diamagnetic Kernel

$$\delta A_h = \frac{\pi e^2 a_\delta^2}{2\hbar^2 \Omega} < -T_\delta^{\Delta t} > . \tag{42}$$

¿From Eqs. (27) and (29), the spectral representation of the paramagnetic London Kernel is

$$K_{1\delta} = \frac{8\pi}{c^2 \Omega Z} \sum_{n,m} \frac{e^{-\beta E_n}}{E_n - E_m} | < n | J_\delta | m > |^2. \tag{43}$$

Finally, we define the sum rule violation parameter in direction δ

$$V_\delta = \frac{\delta A_h^\delta}{\delta A_l^\delta + \delta A_h^\delta} \tag{44}$$

which quantifies the relative amount of sum rule violation.

A. Clean limit

In the absence of disorder the paramagnetic London Kernel is easily evaluated and yields

$$K_{1\delta} = \frac{32\pi e^2 t_\delta a_\delta^2}{\hbar^2 c^2 \Omega} \frac{1}{N} \sum_k sin^2 k_\delta (\frac{\partial f}{\partial E_k}). \tag{45}$$

It is easily seen [3] that at $T = T_c$, $K_{1\delta}$ exactly cancels the single-particle kinetic energy in Eq. (41), hence $\delta A_l = 0$. Similarly $\delta A_h = 0$ since $\Delta_k = 0$. Hence the superfluid weight goes to zero at T_c as expected. In the limit of zero temperature, $K_{1\delta}$ goes to zero and the low frequency missing area Eq. (41) is given by the expectation value of the single particle kinetic energy

$$\delta A_l = \frac{\pi e^2 a_\delta^2}{2\hbar^2 \Omega} < -T_\delta^t > . \tag{46}$$

Hence the sum rule violation parameter is simply

$$V_\delta = \frac{< T_\delta^{\Delta t} >}{< T_\delta^t > + < T_\delta^{\Delta t} >} \tag{47}$$

and can be calculated from Eq. (37).

As we will see in the next section, the in-plane sum rule violation is generally larger than the c-axis one in the clean limit. From Eq. (47), this will be the case if

$$\frac{<T_a^{\Delta t}>}{<T_c^{\Delta t}>} > \frac{<T_a^t>}{<T_c^t>} \tag{48}$$

holds, that is, if the anisotropy in the anomalous part of the kinetic energy is larger than that in the single particle part. This is indeed the case and can be understood both from a strong and a weak coupling argument, as discussed in the following.

From Eq. (37) it would appear that the anisotropy in both $<T_\delta^t>$ and $<T_\delta^{\Delta t}>$ is given by η, Eq. (5), since they have as prefactor t_δ and Δt_δ respectively. However this argument is misleading. In strong coupling, the anomalous kinetic energy is proportional to [3]

$$<T_\delta^{\Delta t}> \sim \frac{(\Delta t_\delta)^2}{U} \tag{49}$$

corresponding to second order processes where a hole hops onto a site already occupied by another hole, with an energy cost U. In contrast, $<T_\delta^t>$ is dominated by first order processes, hence is proportional to t_δ. As a consequence, the anisotropy in $<T_\delta^t>$ will be closer to η and that in $<T_\delta^{\Delta t}>$ closer to η^2.

From a weak coupling point of view we can also understand the different anisotropy Eq. (48) from the expressions for the kinetic energies Eq. (37). The contributions to the sum over k, k' in Eq. (37c) are dominated by values of k, k' in the vicinity of the Fermi surface. Except for extremely small doping, the Fermi surface for the anisotropic band structure has a "cigar" form extending over all values of k_z but only a small range of k_x, k_y close to the origin. For $<T_c^{\Delta t}>$, the factors of $cosk_z$, $cosk_z'$ lead to cancellations because they extend over both positive and negative value, e.g. for k_z and $(\pi - k_z)$, while for $<T_a^{\Delta t}>$ the factors $cosk_x$, $cosk_x'$ have always the same sign. Hence the anisotropy in $<T_\delta^{\Delta t}>$ will in general be substantially larger than η, except for very low doping where the Fermi surface is just small pockets around the points $(0, 0, +/-\pi)$. For $<T_\delta^t>$ instead, Eq. (37b), the contributions to the sum over k do not come only from points around the Fermi surface but from all points inside the Fermi surface. There is also a cancellation here between positive and negative values of $cosk_z$ and hence the anisotropy in $<T_\delta^t>$ is also larger than η. However the cancellation is less complete here because there is more phase space inside the Fermi surface for k_z than there is for $(\pi - k_z)$, for $k_z < \pi/2$. Hence the anisotropy in $<T_\delta^t>$ is smaller than that in $<T_\delta^{\Delta t}>$, as given by Eq. (48), leading to larger in-plane than c-axis sum rule violation.

B. Effect of disorder

In the presence of disorder the weight in the δ-function is decreased and hence the penetration depth increases. Qualitatively this can be seen from the Drude form of the optical conductivity

$$\sigma_1(\omega) = \frac{ne^2\tau}{m^*} \frac{1}{1 + \omega^2\tau^2} \tag{50}$$

with τ the scattering time. Upon entering the superconducting state the optical absorption at frequencies of order $\hbar\omega < 2\Delta$ is suppressed due to the opening of the gap; as the disorder increases, the weight in that frequency range decreases by a factor of order $\Delta/(\hbar/\tau)$, and the penetration depth at low temperatures is given approximately by [20]

$$\frac{1}{\lambda_\delta^2} = (\frac{1}{\lambda_\delta^{clean}})^2 \frac{1}{1 + \frac{\hbar/\tau_\delta}{\pi\Delta}} \equiv \frac{1}{(\lambda_\delta^{clean})^2} p_\delta \tag{51}$$

The detailed calculation within BCS theory is given in Ref. 21 for the jellium model, and in Ref. 22 for arbitrary impurity scattering rate. The diamagnetic London Kernel, given by the expectation value of the single particle kinetic energy, is assumed to be unaffected by disorder. Similarly we expect the expectation value of the pair contribution to the kinetic energy, $<T_\delta^{\Delta t}>$, to be unaffected by disorder as long as it is weak enough not to cause pairbreaking. Under those conditions disorder will only affect the paramagnetic London Kernel, and hence only the low frequency missing area. Since δA_l in Eq. (44) is reduced by disorder and δA_h is unaffected, the sum rule violation will increase, as was shown schematically in Figure 1. In the presence of sum rule violation Eq. (51) becomes

$$\frac{1}{\lambda_\delta^2} = (\frac{1}{\lambda_\delta^{clean}})^2 [p_\delta + V_\delta^{clean}(1 - p_\delta)] \tag{52}$$

and the sum rule violation in the presence of disorder is given by

$$V_\delta = \frac{\delta A_h^\delta}{\delta A_l^\delta \times p_\delta + \delta A_h^\delta} = V_\delta^{clean}(\frac{\lambda_\delta}{\lambda_\delta^{clean}})^2 \tag{53}$$

where the missing areas are understood to be those in the clean limit. The disorder parameter p_δ can be written as

$$p_\delta = [(\frac{\lambda_\delta^{clean}}{\lambda_\delta})^2 - V_\delta^{clean}]\frac{1}{1 - V_\delta^{clean}} \tag{54}$$

so that it can be obtained from our calculated penetration depth and sum rule violation in the clean limit together with the observed value of the penetration depth.

There is substantial experimental evidence that the effect of disorder is substantially stronger for c-axis transport than for in-plane transport in the cuprates in the underdoped regime, i.e. $\tau_c/\tau_a << 1$, and that transport in the planes can be understood within the clean limit [11–13]. As the doping is increased, transport in the c-direction is found to become more coherent, i.e. τ_c increases. The penetration depth in the c-direction will hence be increased compared to its clean limit value, especially in the underdoped regime, and consequently from Eq. (53) the sum rule violation in the c-direction will also be increased. This effect is much larger than the anisotropy in the violation in the clean limit discussed in the previous section. Hence in the presence of disorder the sum rule violation in the c-direction will dominate. As the doping increases we will find that the sum rule violation in the c-direction decreases rapidly, both because the system is approaching the clean limit and because the intrinsic violation in the clean limit also decreases with doping.

IV. RESULTS IN THE CLEAN LIMIT

Much of the behavior of our model is determined by the in-plane physics, that dominates the energetics. Furthermore the properties of the model are not very sensitive to the detailed density of states, and hence it is possible to learn about many of the properties by considering simply a two-dimensional model with constant density of states, as done for example in Refs. [4] and [7]. Here, to compare the behavior of in-plane and c-axis properties we will consider the full anisotropic three-dimensional model at the outset. The in-plane properties of that model are very similar to those of the simpler two-dimensional model.

For definiteness we will assume an on-site Hubbard repulsion $U = 5$ eV, and an anisotropy in hopping and in correlated hopping $\eta = 25$ (Eq. 5). We will show results for a set of bandwidths spanning the weak to strong coupling regime, $D = 1.5$ eV, 1 eV, 0.5 eV, 0.1 eV, and nearest neighbor repulsion $V = 0$ and $V = 0.65$ eV. We expect the actual value of V in the cuprates to be somewhere in-between those two values. The magnitude of the hopping interaction Δt is chosen to yield a maximum T_c of 37.5 K or 90 K. The first is appropiate for $LaSrCuO_4$, the second for $Tl2201$, $Hg1201$ and $YBCO123$ structures.

Figures 2 (a) and (b) show results for the critical temperature versus doping for nearest neighbor repulsion $V = 0$ and maximum T_c of 37.5 K and of 90 K respectively, for the set of bandwidths considered. It can be seen that the results are very similar for all cases considered, except that as the bandwidth decreases the width of the peak increases slightly. On the other hand the condensation energy, shown in Fig. 3, is strongly dependent on the bandwidth and increases as the bandwidth decreases, as would be expected from Eq. (11).

The in-plane sum rule violation Eq. (44) is shown in Fig. 4. In the purely two-dimensional model it is a monotonically decreasing function of doping [7], whereas in the three-dimensional structure it decreases at very low densities in weak coupling, as the density of states goes to zero. The sum rule violation decreases rapidly as the bandwidth increases, and is larger for the cases corresponding to higher T_c.

The behavior of the sum rule violation parameter in the c-direction is similar to the in-plane one but smaller in magnitude, as shown in Fig. 5, in accordance with the discussion in the previous section. The decrease at low densities is somewhat less pronounced than for the in-plane case. In Fig. 6 we plot the sum rule violation anisotropy, V_a/V_c. As the bandwidth increases the sum-rule violation anisotropy increases, and the c-axis sum rule violation can be up to a factor of 5 smaller than the in-plane violation for the parameters considered here.

Next we consider the effect of nearest neighbor repulsion V. The critical temperature versus doping, shown in Fig. 7, shows somewhat larger dependence on bandwidth than the case $V = 0$ but is otherwise similar. The condensation energy, Fig. 8, is somewhat decreased compared to the case $V = 0$ (Fig. 3), (for parameters chosen to yield the same T_c^{max}), particularly as the bandwidth becomes small. On the other hand the in-plane sum rule violation, Fig. 9, increases compared to the case $V = 0$ (Fig. 4) for all the different bandwidths. The anisotropy in the sum rule violation, Fig. 10, shows similar magnitude and doping dependence as the case $V = 0$ (Fig. 6).

These results indicate that the in-plane sum rule violation will be easiest to detect in the underdoped regime, and in cuprates where the condensation energy is large, due to a large density of states (small bandwidth), and where the nearest neighbor Coulomb repulsion is appreciable.

In addition to the sum rule violation, which involves the ratio of kinetic energies, it is useful to consider the behavior of the kinetic energies themselves. Figure 11 shows the behavior of the in-plane kinetic energies versus doping for one case: single-particle contribution (a), pair contribution (b) and total (c). The pair contribution is proportional to the anomalous part of the $\delta-$function response coming from high frequencies, Eq. (36), while the single particle contribution gives the regular part of the $\delta-$function coming from low frequencies, Eq. (46), *in the clean limit.* In the presence of disorder the latter contribution will be reduced, while the former one is expected to remain the same. Finally, the total kinetic energy will be proportional to the total weight in the $\delta-$function and hence the inverse squared penetration depth in the clean limit only.

It can be seen from Fig. 11 that the pair contribution to the kinetic energy is maximum approximately at the same doping where T_c is maximum (optimally doped) for the larger bandwidths, and at even higher doping for small bandwidth. This is in contrast to the sum rule violation parameter that decreases monotonically from the underdoped through the overdoped regime. That is, we predict that the anomalous kinetic energy contribution should persist well into the overdoped regime. Experimentally this effect may be difficult to detect because the normal contribution increases rapidly with doping and will strongly dominate the superfluid weight in the overdoped regime. This effect will be even more pronounced if, as we expect, the effect of disorder becomes less pronounced as the doping increases. This will be further discussed in the following section.

The behavior of the kinetic energies in the z-direction is similar, as seen in Fig. 12. In Fig. 13 we show the anisotropy in the normal and anomalous parts of the kinetic energy. In accordance with the discussion in the previous section, both are larger than the anisotropy in the hopping, η, and they increase with dooping. Fig. 14 shows the resulting anisotropy in the total kinetic energy, which in the clean limit is inversely proportional to the square of the anisotropy in the penetration depths. For all except the smallest bandwidth, the doping dependence obtained is opposite to what is observed experimentally e.g. in $LaSrCuO$, where the anisotropy in penetration depths is found to decrease as the doping increases. We attribute this discrepancy to a variation of the effect of disorder with doping [12], as will be discussed in the next section.

Within a simple two-fluid picture with parabolic bands one would expect the anisotropy in the kinetic energies or the clean limit squared penetration depths to be given by the effective mass anisotropy,

$$\frac{< T_a >}{< T_c >} = \frac{\lambda_c^2}{\lambda_a^2})_{clean} = \frac{m_c^*}{m_a^*} = \frac{t_a}{t_c} \tag{55}$$

which for the case considered here is 25. From Fig. 14 it can be seen that this value is in fact only approached in the weak coupling regime (large bandwidth) and for small doping. As the doping increases the anisotropy increases rapidly, and for the case of strong coupling (small bandwidth) the anisotropy also increases in the underdoped regime. In fact in the strong coupling limit the anisotropy in the kinetic energies will approach the square of the band structure anisotropy. The anisotropy in penetration depths will furthermore be increased even further due to the effect of disorder, as will be discussed in the next section.

Finally, it is interesting to consider the various different contributions to the condensation energy. Figure 15 shows results for a two-dimensional case, for parameters appropiate to mimic the in-plane behavior of the three-dimensional model for parameters corresponding to the case of Figures (12-14) for bandwidths 1 eV and 0.1 eV. All contributions to the condensation energy are negative except the one corresponding to the correlated hopping term, which is about 50 times larger than the condensation energy. Quite generally the kinetic energy lowering in our model due to the pair hopping contribution is much larger than the condensation energy and is partially compensated by an increase in Coulomb repulsion in the paired state, because carriers in the pair are on average closer to each other than in the normal state. Note from Fig. 13 that the kinetic energy lowering from c-axis motion is a small fraction of the kinetic energy lowering from in-plane motion, in contrast to the prediction of the interlayer tunneling theory [8].

In summary, we have seen in this section that for a given value of maximum T_c the model can yield a fairly wide range of values of condensation energy and sum rule violation depending on parameters in the Hamiltonian. Still, the systematics with doping is always the same, as is the fact that the in-plane sum rule violation is always larger than the c-axis one. The magnitude of the condensation energy for given maximum T_c decreases monotonically as the bandwidth increases (i.e. density of states decreases) for any doping. In Fig. 16 we show the bandwidth dependence for the optimally doped case and $T_c^{max} = 90K$. As seen in Fig. 16, the effect of nearest neighbor repulsion is to decrease somewhat the condensation energy. Both the in-plane and interplane sum-rule violation decrease as the bandwidth increases, and the effect of nearest neighbor repulsion is to increase the degree of sum-rule violation, as shown in Fig. 17. The violation is always larger in-plane than out of plane, and the anisotropy in the violation increases as the bandwidth increases except in the very overdoped regime.

V. COMPARISON WITH EXPERIMENT

It is generally accepted that in-plane transport in the cuprates is described by the clean limit, and here we adopt this point of view. To determine the parameters appropiate to the different materials we use results for the condensation energy obtained by Loram [24] from analysis of specific heat data. Loram reports a maximum condensation energy $U_0 = 3.6 J/g - at$ for $YBCO$, $U_0 = 2.8 J/g - at$ for $YBCO$ with 20% Ca substituting for Y, $U_0 = 2 J/g - at$ for $Bi2212$, and $U_0 = 1.3 J/g - at$ for $LaSrCuO_4$. If we assume that the condensation energy is dominated by the physics of the planar oxygens, we have per planar oxygen a condensation energy ϵ_c given by

$$\epsilon_c(\mu eV) = U_0(\frac{Joule}{g - at}) \times 5.18 \times \frac{N_1}{N_2} \tag{56a}$$

$$N_1 = number\ of\ atoms\ in\ formula\ unit \tag{56b}$$

$$N_2 = number\ of\ planar\ CuO_2's\ in\ formula\ unit \tag{56c}$$

yielding $\epsilon_c = 121\mu eV$ for $YBCO$ ($N_1 = 13$, $N_2 = 2$), $\epsilon_c = 78\mu eV$ for $Bi2212$ ($N_1 = 15$, $N_2 = 2$), $\epsilon_c = 94\mu eV$ for $Y_{0.8}Ca_{0.2}Ba_2Cu_3O_{6+y}$, and $\epsilon_c = 47\mu eV$ for $LaSrCuO$ ($N_1 = 7$, $N_2 = 1$). Assuming a value for the nearest neighbor repulsion we can then extract the required value of the bandwidth by inspection of Fig. 16.

It can be seen that the maximum condensation energy for the various materials with $T_c^{max} \sim 90$ K coincide within a factor of 2. Differences may be due to contributions to the condensation energy from other atoms in the structure besides the CuO_2 units. We will assume that a proper value for the bandwidth in our model to describe a $T_c^{max} \sim 90$ K material is $D = 0.5$ eV, which yields a maximum condensation energy in the range of values given above, for reasonable values of the nearest neighbor repulsion. Figure 18 shows the condensation energy versus doping for values of the nearest neighbor repulsion $V = 0$ and $V = 0.65$ eV. The maximum condensation energy is $\epsilon_c = 104\mu eV$ and $\epsilon_c = 90\mu eV$ respectively. For $LaSrCuO$, the condensation energy reported by Loram is somewhat larger than expected if the same bandwidth is assumed as for the $90K$ materials, since Eq. (11) (assuming equal gap ratios) would predict a condensation energy ~ 6 times smaller for $LaSrCuO$. If Loram's values are accurate it would imply within our model a bandwidth of $D \sim 0.25$ eV for $LaSrCuO$, which would give rise to a substantial sum rule violation even in the clean limit, as seen in the previous section.

A. Effect of disorder

We choose the case of $YBCO$ for a detailed comparison with experiment, since experimental results for the sum rule violation for several values of doping [6] are available only for this material. ¿From band structure calculations [25] we extract for the band structure anisotropy $t_a/t_c = 10$. Figure 19 shows the calculated values for the sum rule violation in the a and c directions in the clean limit for this case. For definiteness we will consider in what follows the case of zero nearest neighbor repulsion. For the c direction we also show the experimental values measured by Basov et al [6]. We chose to assign to the samples in Basov's experiments the value of doping that would give rise to the same critical temperature in our model as seen experimentally. The results in Fig. 19b show that experiments exhibit a much faster decrease in the sum rule violation with doping than our clean-limit calculation predicts.

However, as mentioned earlier there exists substantial experimental evidence pointing to the fact that transport in the c-direction is described by the dirty rather than the clean limit [11,12,14,13]. Furthermore, transport [26] as well as optical [12] experiments indicate that the c-axis scattering rate decreases rapidly as the doping increases. This has been modeled theoretically [27] taking into account diagonal and off-diagonal disorder, and assuming that Coulomb effects cause both the in-plane and interplane hopping amplitudes to increase with doping. This latter assumption is in fact the basis of our model, i.e. Eq. (1). These experiments and calculations suggest that the c-axis transport evolves from the dirty towards the clean limit as the doping increases. As we show in what follows, this is in fact consistent with the predictions of our model, and leads to a faster rate of decay of the c-axis sum rule violation with doping than in the clean limit, consistent with observations.

The penetration depths at zero temperature are related to the kinetic energies by

$$\lambda_a(\mathring{A}) = 4638(d(\mathring{A}))^{1/2}\frac{1}{(T_a(meV))^{1/2}} \tag{57a}$$

$$\lambda_c(\mathring{A}) = 4638(\frac{a(\mathring{A})^2}{d(\mathring{A})})^{1/2}\frac{1}{(T_c(meV))^{1/2}}. \tag{57b}$$

The in-plane kinetic energy obtained from our model for the parameters under consideration and optimal doping is $T_a = 6.6$ meV (per oxygen site). It is not completely clear what the parameter d in Eq. (57a) should be. If we assume that only the oxygens in the CuO planes contribute to the penetration depth, we should take for d one-half of the c-axis lattice constant $d = 11.68\mathring{A}$, which yields from Eq. (57a) an in-plane penetration depth $\lambda_a \sim 4300\mathring{A}$. This is substantially larger than the observed penetration depth, $\lambda_a \sim 1400\mathring{A}$ [28], and suggests that carriers from other atoms in the structure also contribute to the superfluid weight. We will simply treat d in Eq. (57a) as a parameter to be determined to fit the observed penetration depth in the optimally doped case. For Eq. (57b) we will use the YBCO lattice constants $a = 3.84\mathring{A}$ and $d = 11.68\mathring{A}$.

Figure 20 shows calculated values of the penetration depth and experimental observations [28,6]. Again we infer the appropiate values of n for the experimental data by comparison of experimental and calculated T_c/T_c^{max}. The in-plane calculated penetration depth for small doping becomes somewhat larger than the experimental one. The discrepancy may arise from contribution to the superfluid weight from carriers in other bands with weaker carrier concentration dependence with doping than the oxygen band described by our model [15].

The calculated penetration depth in the c direction increases much more slowly than the experimental one as the doping decreases. We attribute this to an enhanced effect of disorder in the c-axis transport in the underdoped regime. This is in fact consistent with interpretation of optical experiments in LaSrCuO [12] indicating a stronger c-axis scattering rate in the underdoped regime, as well as with transport experiments in YBCO [26]. By comparison of calculated and observed penetration depth anisotropies, shown in Fig. 21, we extract the doping dependence of the c-axis scattering rate in Eq. (51):

$$(1 + \frac{\hbar/\tau_c}{\pi\Delta})^{-1} \equiv p_c = \frac{(\lambda_c/\lambda_a)^2_{theory,cleanlimit}}{(\lambda_c/\lambda_a)^2_{experiment}}. \tag{58}$$

This assumes that the penetration depth in the plane is described approximately by the clean limit result given by our calculation. The c-axis scattering rate thus obtained has a strong doping dependence.

We can hence calculate the doping dependence of the c-axis sum rule violation in the presence of disorder, as determined by Eq. (53):

$$V_c = V_c^{clean}(\frac{\lambda_c}{\lambda_c^{clean}})^2 = V_c^{clean}p_c^2 \tag{59}$$

and plot the results in Fig. 22, together with experimental observations [6]. The reported experimental error in the sum rule violation parameter is approximately 10% [30]. It can be seen that the theoretical results now show a much stronger variation with doping than in the absence of disorder, and are closer to the experimental observations. A similar analysis was recently given for $LaSrCuO_4$ [29].

B. Kinetic energy lowering

If instead of considering the relative amount of sum rule violation we consider the absolute amount of kinetic energy lowering, we need not worry about the effect of disorder. The amount of kinetic energy in the zero-frequency δ-function is given by

$$Q_\delta = \frac{2\hbar^2 v}{\pi e^2 a_\delta^2}D_\delta = \frac{\hbar^2 c^2 v}{4\pi e^2 a_\delta^2}\frac{1}{\lambda_\delta^2}. \tag{60}$$

with v the volume per CuO_2 planar unit. The kinetic energy lowering is obtained from the experimentally measured penetration depth and sum rule violation as

$$\Delta Q_\delta = Q_\delta V_\delta. \tag{61}$$

In particular, for the c-direction

$$\Delta Q_c = Q_c V_c \tag{62a}$$

$$Q_c = \frac{\hbar^2 c^2 a^2}{4\pi e^2 d}\frac{1}{\lambda_c^2} \tag{62b}$$

12

For YBCO, with two CuO_2 planes per unit cell, we take d as half the unit cell dimension in the c-direction, and Eq. (62b) gives the kinetic energy per CuO_2 planar unit.

Basov and coworkers reported values for V_c for $YBCO$ for several dopings, for $Tl2201$ for an optimally doped and one overdoped sample, and for slightly underdoped $LaSrCuO$, together with the corresponding c-axis penetration depths [6]. Furthermore, Basov reports an error of approximately 10% for the reported value of $(1 - V_c)$ [30]. We can then obtain the experimentally observed absolute value of kinetic energy lowering from Eq. (62), and the associated error from

$$\delta(\Delta Q_c) \sim 0.1 Q_c \tag{63}$$

assuming the relative error in the measured penetration depth is much smaller than in the sum rule violation. Table I summarizes Basov's results and the resulting values for kinetic energy lowering from Eqs. (62) and (63).

In our model, the kinetic energy lowering is given by the expectation value of the correlated hopping term $< T_\delta^{\Delta t} >$. Since there are two O atoms per CuO_2 unit, we have

$$\Delta Q_c)_{theory} = 2 < T_\delta^{\Delta t} > \tag{64}$$

since our calculated kinetic energy lowering is per O atom.

We estimate hopping anisotropies from band structure calculations to be approximately $t_a/t_c = 10$ for $YBCO$ [25], 25 for $LaSrCuO$ [25], and 50 for $Tl2201$ [31]. In the latter it should be noted this is estimated to be the average anisotropy for all bands, while for the $Cu - O$ band alone it is estimated to be about 600. According to our estimates from the previous subsection we assume bandwidths $D = 0.5$ eV for $YBCO$ and $Tl2201$, and $D = 0.25$ eV for $LaSrCuO$. In Fig. 23 we plot the observed and calculated values of kinetic energy lowering. For $LaSrCuO$, we use a non-zero nearest neighbor repulsion in order to fit the rather large value of kinetic energy lowering observed. It can be seen that our calculation gives reasonable agreement with experimental measurements in the underdoped regime. In the optimally doped and overdoped regimes our calculation predicts a significant kinetic energy lowering, but unfortunately experimental errors are at present too large to confirm or rule out our predictions.

VI. SUMMARY AND CONCLUSIONS

The sum rule violation considered here has also been discussed by other workers. Kim [32] considered the role of impurity scattering in c-axis transport for a $d_{x^2-y^2}$ gap and concluded that the superfluid weight could be both larger or smaller than the missing area in the conductivity depending on parameters. Ioffe and Millis [33] argued that the explanation of Basov's observations lies in the interplay of phase coherence, quantum and thermal fluctuations, and scattering processes. Neither of these treatments predicts an in-plane sum rule violation, in contrast to our model. Kim and Carbotte [34] found that if there is coherent interlayer coupling there should be no c-axis sum rule violation; their model however did not include a correlated hopping term. Furthermore they found that for incoherent interlayer coupling there should be sum rule violation, however of opposite sign to that observed. Within their model (without a Δt term) they found that in-plane sum rule violation (of either sign depending on parameters) can occur only if the electronic density of states has fine structure on the scale of the superconducting gap.

In summary, we have studied here the predictions of the model of hole superconductivity for the condensation energy and for quantities related to the optical sum rule, for a wide range of parameters. The model predicts a violation of the Ferrell-Glover-Tinkham sum rule that can range from a few percent to close to 100% depending on the parameters in the Hamiltonian. For given maximum T_c, the most important parameter determining the magnitude of sum rule violation is the bandwidth, or density of states: larger density of states gives rise to larger sum rule violation, as well as to larger condensation energy. Comparison of calculated and measured condensation energy for a given system allows for a determination of the parameters in the Hamiltonian appropiate for that system.

The transition to the superconducting state is driven by lowering of kinetic energy for all dopings in this model. Quite generally, the lowering of kinetic energy is one to two orders of magnitude larger than the superconducting condensation energy. Because the condensation energy peaks approximately at the same doping as T_c, the model predicts a substantial kinetic energy lowering in the overdoped regime. For the anisotropic structures of the cuprates, the contribution to the condensation energy from in-plane kinetic energy lowering is two to three orders of magnitude larger than that of interplane motion.

Furthermore the model predicts that in the clean limit the in-plane sum rule violation should be a few times larger than the interplane one. The fact that the opposite has been reportedly observed so far [6] (large c-axis violation, no in-plane violation) leads us to conclude that there is a significant effect of disorder in c-axis transport, that suppresses the low frequency spectral weight and hence allows for easier detection of the anomalous high frequency spectral

weight. This assumption is in fact consistent with a variety of other experimental observations [11–14], that have led several workers to conclude that c-axis transport is described by the dirty limit and planar transport by the clean limit. Using this assumption our model can explain the large difference between observed c-axis and in-plane sum rule violations.

Furthermore, comparison of our calculated and measured c-axis penetration depths led us to conclude that the effect of disorder in c-axis transport increases substantially in the underdoped regime. This conclusion is also in fact consistent with other independent experimental observations [12,26]. This fact leads to a much more rapid doping dependence of the sum rule violation than that obtained in the clean limit, which resembles the experimental observations [6].

Experimental papers have suggested that the sum rule violation effect disappears in optimally doped or overdoped regime, and concluded from this that there is no anomalous kinetic energy lowering in those regimes [6]. We argue that this conclusion is flawed. Because the 'normal' contribution to the superfluid weight increases rapidly as the doping increases, it can easily mask the anomalous part of the superfluid weight, which has, according to our calculation, a much slower doping dependence and decreases slowly in the overdoped regime. In experimental papers [6] it is always the fractional sum rule violation that is plotted, rather than the absolute value of kinetic energy lowering. This is presumably due to the fact that large error bars prevent meaningful extraction of the latter quantity. However it should then be recognized that an apparent vanishing of the fractional sum rule violation within error bars does not imply a vanishing of the anomalous kinetic energy lowering.

There is another fundamental reason to reject this experimental conclusion. If there is indeed the unusual phenomenon of kinetic energy lowering, contrary to ordinary BCS theory, it is logical to conclude that whatever mechanism is causing the kinetic energy lowering drives the transition to superconductivity, and that the lowering of kinetic energy is responsible for the condensation energy of the superconductor. At present both our calculations and experiments [24] indicate that the condensation energy in the cuprates as a function of doping peaks in the optimally doped or even overdoped regimes. If there is no kinetic energy lowering in the optimally doped or overdoped regimes, as proposed by Basov, it would imply that a different mechanism explains superconductivity in those regimes. Moreover, the kinetic energy lowering mechanism would apply for optimally doped $Tl_2Ba_2CuO_{6+\delta}$ but not to optimally doped $YBa_2Cu_3O_x$ according to Basov's point of view. Clearly, while such a scenario would not be impossible, it does not appear to be very plausible.

In this paper we have not discussed the temperature dependence of these effects. So far, no experimental results have been reported for the temperature dependence of missing areas and sum rule violation. We have discussed elsewhere for selected cases the temperature dependence of the real part of the conductivity [35], London penetration depth [3] and high and low frequency missing areas [4] within our model. Once experimental results for these quantities become available it will be possible to provide detailed comparison with the theory.

In conclusion we note that the mechanism of hole superconductivity discussed here is the only mechanism of superconductivity so far proposed that both predicts an optical sum rule violation due to kinetic energy lowering, and allows for quantitative evaluation of the doping and temperature dependence of the effect. Existing experiments confirm the existence of the c-axis sum rule violation, and suggest that kinetic energy lowering also occurs in in-plane transport [36,6], in agreement with the predictions of the model. Future more accurate experiments should be able to provide more stringent tests of the theory. Furthermore, the model of hole superconductivity is the only one proposed so far that provides an explanation for the origin of the high frequency spectral weight that appears in the zero-frequency delta-function [19]. It remains a challenge for other theories to provide explanations for these unusual experimental observations.

ACKNOWLEDGMENTS

[1] J.E. Hirsch and F. Marsiglio, Phys. Rev. B **39**, 11515 (1989); Physica C **162-164**, 591 (1989); F. Marsiglio and J.E. Hirsch, Phys. Rev. B **41**, 6435 (1990).
[2] J. E. Hirsch, Physica C **158**, 326 (1989); Phys.Rev. B**48**, 9815 (1993).

[3] J. E. Hirsch and F. Marsiglio, Phys. Rev. B **45**, 4807 (1992).

[4] J. E. Hirsch, Physica C **199**, 305 (1992).

[5] R.A. Ferrell and R.E. Glover, Phys. Rev **109**, 1398 (1958) ; M. Tinkham and R.A. Ferrell, Phys.Rev.Lett. **2**, 331 (1959).

[6] D.N. Basov et al, Science **283**, 49 (1999); A.S. Katz et al, Phys.Rev. B **61**, 5930 (2000); D.N. Basov et al, preprint.

[7] J.E. Hirsch and F. Marsiglio, cond-mat/9908322, Physica C **331**, 150 (2000).

[8] P.W. Anderson, 'The Theory of Superconductivity in the High T_c cuprates", Princeton University Press, Princeton, 1997; Science **268**, 1154 (1995); Science **279**, 1196 (1998).

[9] S. Chakravarty, Eur.Phys.J. B**5**, 337 (1998); S. Chakravarty, H.Y. Young and E. Abrahams, Phys.Rev.Lett. **82**, 2366 (1999).

[10] A.A. Tsvetkov et al, Nature **395**, 360 (1998); J. Schutzmann et al, Phys. Rev. B **55**, 11118 (1997); K.A. Moler et al, Science **279**, 1193 (1998).

[11] D. Van der Marel and J.H. Kim, J. Phys. Chem. Solids **56**, 1825 (1995).

[12] S.Uchida, K. Tamasaku and S. Tajima, Phys.Rev.B **53** , 14558 (1996).

[13] T. Shibauchi et al, Phys.Rev.Lett. **72**, 2263 (1994).

[14] S. Tajima et al, Phys. Rev. B **55**, 6051 (1997).

[15] These orbitals can also be taken into account but do not modify the essential physics: J.E. Hirsch and F. Marsiglio, Phys.Rev.B **43** , 424 (1991).

[16] Actually, in many cases the approximation alluded to (discussed in detail in the third of Refs. [1]) is exact (for example, when $V = 0$).

[17] G.D. Mahan, 'Many-Particle Physics', Plenum, New York, 1981.

[18] P.F. Maldague, Phys.Rev.B **26** , 2437 (1977).

[19] J. E. Hirsch, Physica C **201**, 347 (1992); in "Polarons and Bipolarons in high-T_c Superconductors and Related Materials", ed. by E.K.H. Salje, A.S. Alexandrov and W.Y. Liang, Cambridge University Press, Cambridge, 1995, p. 234 .

[20] M. Tinkham, 'Introduction to Superconductivity', Mc Graw Hill, New York, 1996.

[21] D.C. Mattis, J. Bardeen, Phys. Rev. **111**, 412 (1958).

[22] See, for example, F. Marsiglio, J.P. Carbotte, A. Puchkov and T. Timusk, Phys. Rev. B **53**, 9433 (1996).

[23] F. Marsiglio and J.E. Hirsch, Physica C **165**, 71 (1990).

[24] J. Loram et al, Jour.Phys.Chem. Solids **59**, 2091 (1998); Physica C **282-287**, 1405) (1987); Physica C **235**, 134 (1994); private communication.

[25] P.B. Allen, W.E. Pickett and H. Krakauer, Phys.Rev.B **37**, 7482 (1988).

[26] K. Takenaka et al, Phys. Rev. B **50**, 6534 (1994).

[27] A.G. Rojo and K. Levin, Phys. Rev. B **48**, 16861 (1993).

[28] C. Panagopoulos, J.R. Cooper and T. Xiang, Phys.Rev.B **57**, 13422 (1998).

[29] F. Marsiglio and J.E. Hirsch, presented at the 6th International Conference on Materials and Mechanisms of Superconductivity and High-Temperature Superconductors, Houston, Texas, February 2000, to be published in Physica C.

[30] D.N. Basov, private communication.

[31] D.J. Singh and W.E. Pickett, Physica C**203**, 193 (1992).

[32] E.H. Kim, Phys. Rev. B **58**, 2452 (1998).

[33] L.B. Ioffe and A.J. Millis, Phys. Rev. B **61**, 9077 (2000).

[34] W. Kim and J.P. Carbotte, cond-mat/0003132.

[35] F. Marsiglio and J.E. Hirsch, Phys. Rev. B **44**, 11960 (1991).

[36] S. Uchida, reported at the APS March meeting, March 2000.

TABLE I. Experimental results for c-axis transport, from Ref. 6.

Material	$T_c(K)$	T_c/T_c^{max}	$\lambda_c(A)$	$1 - V_c$	$Q_c(\mu eV)$	$\Delta Q_c(\mu eV)$
$YBa_2Cu_3O_{6+\delta}$						
$\delta = 6.5$	50	0.53	77,350	0.2	9.08	7.26+/- 0.18
$\delta = 6.6$	60	0.64	63,400	0.37	13.5	8.51+/- 0.50
$\delta = 6.7$	65	0.70	51,500	0.87	20.5	2.66+/- 1.8
$\delta = 6.8$	80	0.86	35,000	0.77	44.3	10.2+/- 3.4
$\delta = 6.85$	85	0.91	30,940	1	56.7	0+/- 5.7
$\delta = 6.9$	90	0.96	15,400	1	229	0+/- 23
$\delta = 6.95$	93.5	1	10,300	1	512	0+/- 51
$Tl2201$						
opt. doped	81	1	119,000	0.5	1.99	1.0+/- 0.20
overdoped	32	0.40	110,000	0.9	2.33	0.23+/- 0.21
$LaSrCuO_4$	32	0.85	50,000	0.4	18.6	11.2+/- 0.7

FIG. 1. Sketch of the real part of the conductivity in the superconducting (dashed lines) and normal state (solid lines). The delta function at the origin is the superfluid weight D that determines the London penetration depth. Additional weight is present in the delta function in the superconducting state that originates at high frequency in the normal state. Note that in the dirty limit the contribution to the delta function originating at low frequencies is reduced, and hence the additional weight from high frequencies represents a substantially larger fraction of the delta function. This figure is discussed in detail in section III.

FIG. 2. Critical temperature T_c vs hole concentration n for various bandwidths. In all cases we used $U = 5$ eV, $V = 0$, and $\eta = 25$ for the band anisotropy. The parameter Δt was determined to give (a) $T_c^{\mathrm{max}} = 37.5$ K and (b) $T_c^{\mathrm{max}} = 90$ K. For bandwidths $D = 1.5eV, 1eV, 0.5eV, 0.1eV$ the values of Δt used, in eV, are (a) $\Delta t = 0.295, 0.263, 0.215, 0.141$ and (b) $\Delta t = 0.318, 0.286, 0.240, 0.173$ respectively

FIG. 3. Condensation energy, ϵ_{cond} per planar oxygen, vs. hole concentration for the same parameters as in Fig. 2. The condensation energy decreases with increasing bandwidth, and peaks at roughly the same doping level at which T_c peaks.

FIG. 4. The in-plane sum rule violation, V_a, Eq. (44), vs. hole concentration, for the same cases as in the two previous figures. Except for a small doping level near zero, the violation parameter decreases to zero as hole doping increases. The magnitude of the violation increases as the bandwidth decreases, and is larger when the maximum T_c is larger.

FIG. 5. The out-of-plane sum rule violation, V_c, vs. hole concentration, for the same cases as in the three previous figures. The violation is smaller than the in-plane violation, but otherwise very similar.

FIG. 6. The sum rule violation anisotropy, V_a/V_c, which results from the previous two figures, as a function of hole doping. The anistropy tends to increase as the bandwidth increases, reaching a value of 5 for the cases considered here. The anisotropy is smaller for the case of larger T_c^{max}.

FIG. 7. Critical temperature T_c vs hole concentration n for various bandwidths, as in Fig. 2, but now for $V = 0.65$ eV. As before, $U = 5$ eV and $\eta = 25$ for the band anisotropy. The detailed dependence on bandwidth is more pronounced than with $V = 0$. Again the parameter Δt was determined to give (a) $T_c^{\mathrm{max}} = 37.5$ K and (b) $T_c^{\mathrm{max}} = 90$ K. For bandwidths $D = 1.5eV, 1eV, 0.5eV, 0.1eV$ the values of Δt used, in eV, are (a) $\Delta t = 0.517, 0.503, 0.486, 0.470$ and (b) $\Delta t = 0.533, 0.518, 0.500, 0.483$ respectively.

FIG. 8. Condensation energy vs. hole concentration, as in Fig. 3, but with the same parameters as in Fig. 7 (i.e. with $V = 0.65$ eV). The condensation energy is decreased compared to the $V = 0$ case in Fig. 3.

FIG. 9. The in-plane sum rule violation, V_a, vs. hole concentration, for $V = 0.65$ eV. The magnitude of the violation is significantly increased in comparison to the $V = 0$ case (Fig. 4).

FIG. 10. The sum rule violation anisotropy, V_a/V_c, for $V = 0.65$ eV. The results are similar to the $V = 0$ case (Fig. 6).

FIG. 11. The in-plane kinetic energy (per planar oxygen) vs. doping for the case with $T_c^{\mathrm{max}} = 90$ K and $V = 0.65$ eV. We show (a) the single-particle contribution, (b) the pair contribution, and (c) the total. The single-particle contribution increases with increasing bandwidth and dominates the pair contribution, which decreases with increasing bandwidth. Note that the pair contribution peaks close to the maximum T_c, while the single particle contribution increases monotonically with doping.

FIG. 12. The out-of-plane kinetic energy vs. doping for the same case as in Fig. 11. The results are similar to the in-plane kinetic energy.

FIG. 13. The anisotropy of the single particle (a) and pair contribution (b) to the kinetic energy for the same case as in Fig. 11.

FIG. 14. The anisotropy of the total kinetic energy for the same case as in Fig. 11. The anisotropy is proportional to η at low hole densities in the weak coupling limit. At higher densities, the anisotropy is proportional to η^2 in weak coupling and rises rougly in proportion to hole density. In strong coupling, the anisotropy is proportional to η^2 for all hole densities.

FIG. 15. Various contributions to the condensation energy, using two cases from Figs. (11-14), one with bandwidth (a) $D = 1.0$ eV, and one with bandwidth (b) $D = 0.1$ eV. For simplicity we used a two-dimensional case, with a constant density of states, and Δt re-determined to give $T_c^{\max} = 90$ K. The parameters in the two-dimensional model used to yield the same density of states at the Fermi level and condensation energy as the three-dimensional model for these cases are: (a) $D = 1.6eV$, $\Delta t = 0.51eV$ and (b) $D = 0.25eV$, $\Delta t = 0.48eV$.

FIG. 16. Condensation energy vs. bandwidth for two values of V for the optimally doped case (with $T_c^{\max} = 90$ K). A non-zero nearest neighbour repulsion tends to decrease the condensation energy for a fixed value of T_c^{max}.

FIG. 17. The (a) in-plane, and (b) out-of-plane sum rule violation as a function of bandwidth, for the same two cases as in Fig. 16. The sum rule violation tends to increase with increasing V.

FIG. 18. The condensation energy vs. doping for a specific case: $D = 0.5$ eV, $U = 5$ eV, $T_c^{\max} = 90$ K, for two values of V. $\Delta t = 0.241eV$ for $V = 0$, $\Delta t = 0.501eV$ for $V = 0.65eV$. The T_c curves are also shown to facilitate a comparison of peak positions.

FIG. 19. The (a) in-plane, and (b) out-of-plane sum rule violation as a function of doping for the two cases in Fig. 18. In Fig. (19b) we include for comparison the experimental data from $YBCO$ from Basov $et\ al.$ [6].

FIG. 20. The (a) in-plane, and (b) c-axis, penetration depth, as a function of hole doping, using the case from the previous two figures with $V = 0$. As the doping decreases the experimental data [28] in (b) increases much more quickly than the theoretical clean limit result.

FIG. 21. The ratio of the penetration depths vs. hole doping, along with the experimental results [28], used to determine the impurity parameter, p_c (Eq. (56)).

FIG. 22. The c-axis sum rule violation vs. doping, together with the experimental results [6]. The agreement with experiment is satisfactory, once the stronger c-axis impurity scattering and its doping dependence is accounted for.

FIG. 23. The anomalous contribution to the out-of-plane kinetic energy, for (a) YBCO, (b) Tl2201, and (c) LSCO, plotted along with data from Basov [6]. Note that the error bars become very large as the doping increases (particularly in (a), where two of them exceed the page size). Representative values of the band structure anisotropy are shown in each case. The results are qualitatively consistent with the data, within the error. $\Delta t = 0.240eV$ for (b), $0.477eV$ for (c).
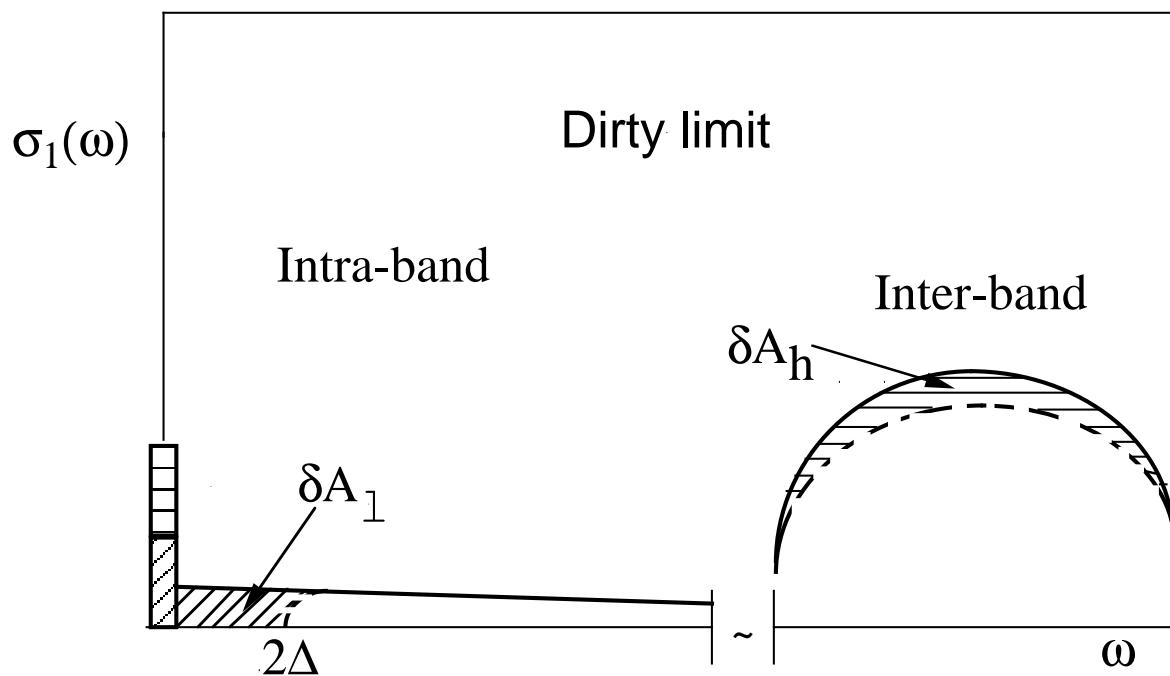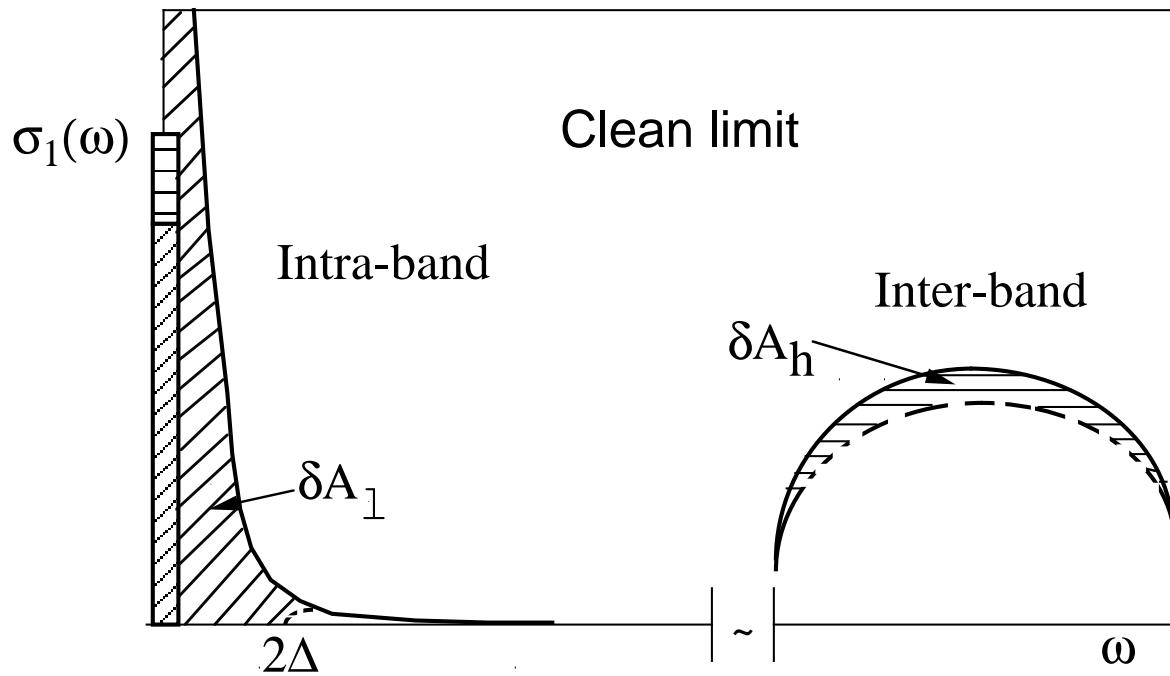
fig2a
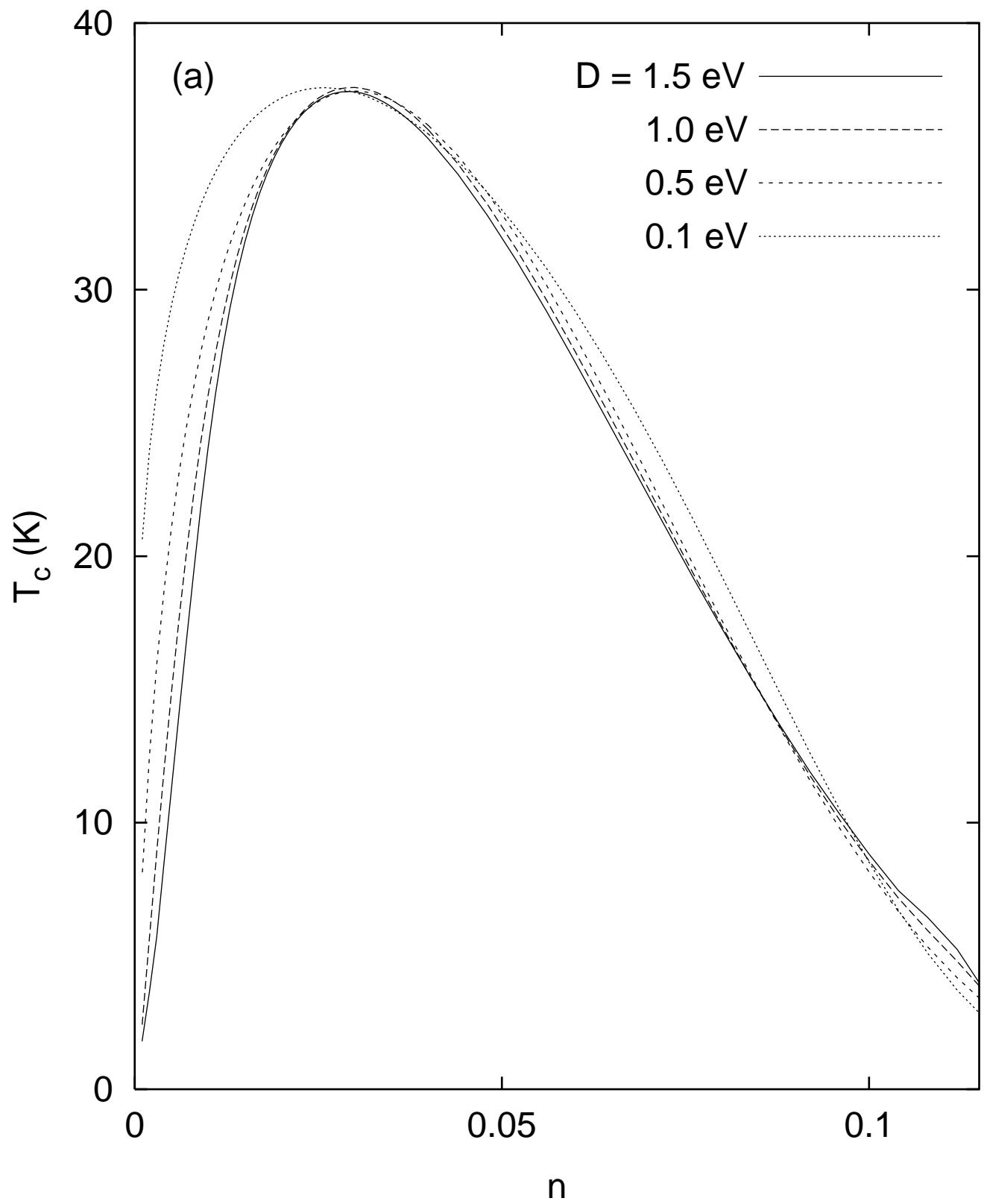
fig2b
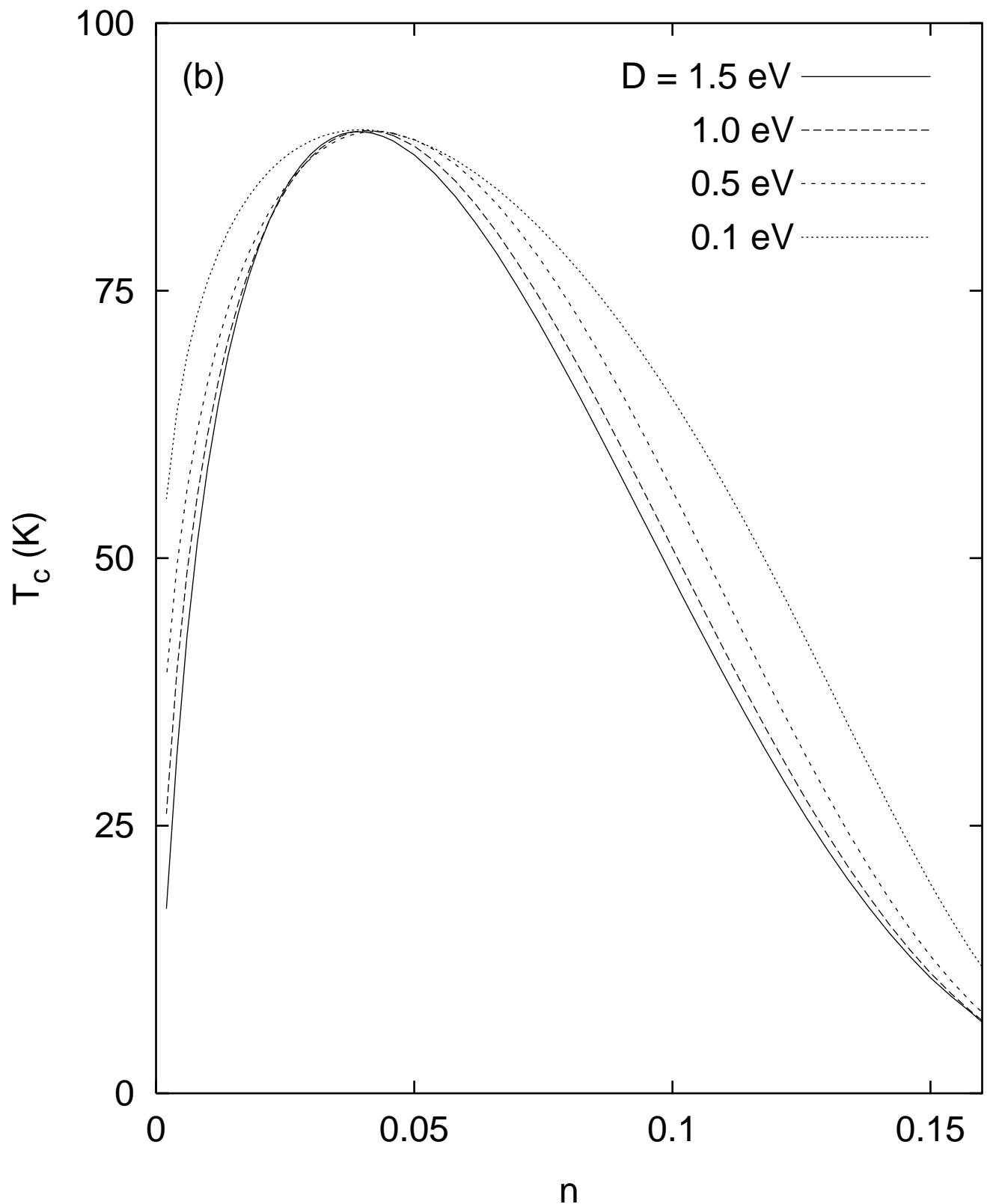
fig3a

fig3b

fig4a

fig4b

fig5a

(a)

V_c

n

D = 1.5 eV
1.0 eV
0.5 eV
0.1 eV

$T_c^{max} = 37.5$ K

0.3

0.2

0.1

0

0.05

0.1

fig5b

(b)

$D = 1.5$ eV
1.0 eV
0.5 eV
0.1 eV

$T_c^{max} = 90$ K

fig6a

(a)

V_a/V_c

$T_c^{max} = 37.5$ K

D = 1.5 eV
1.0 eV
0.5 eV
0.1 eV

n
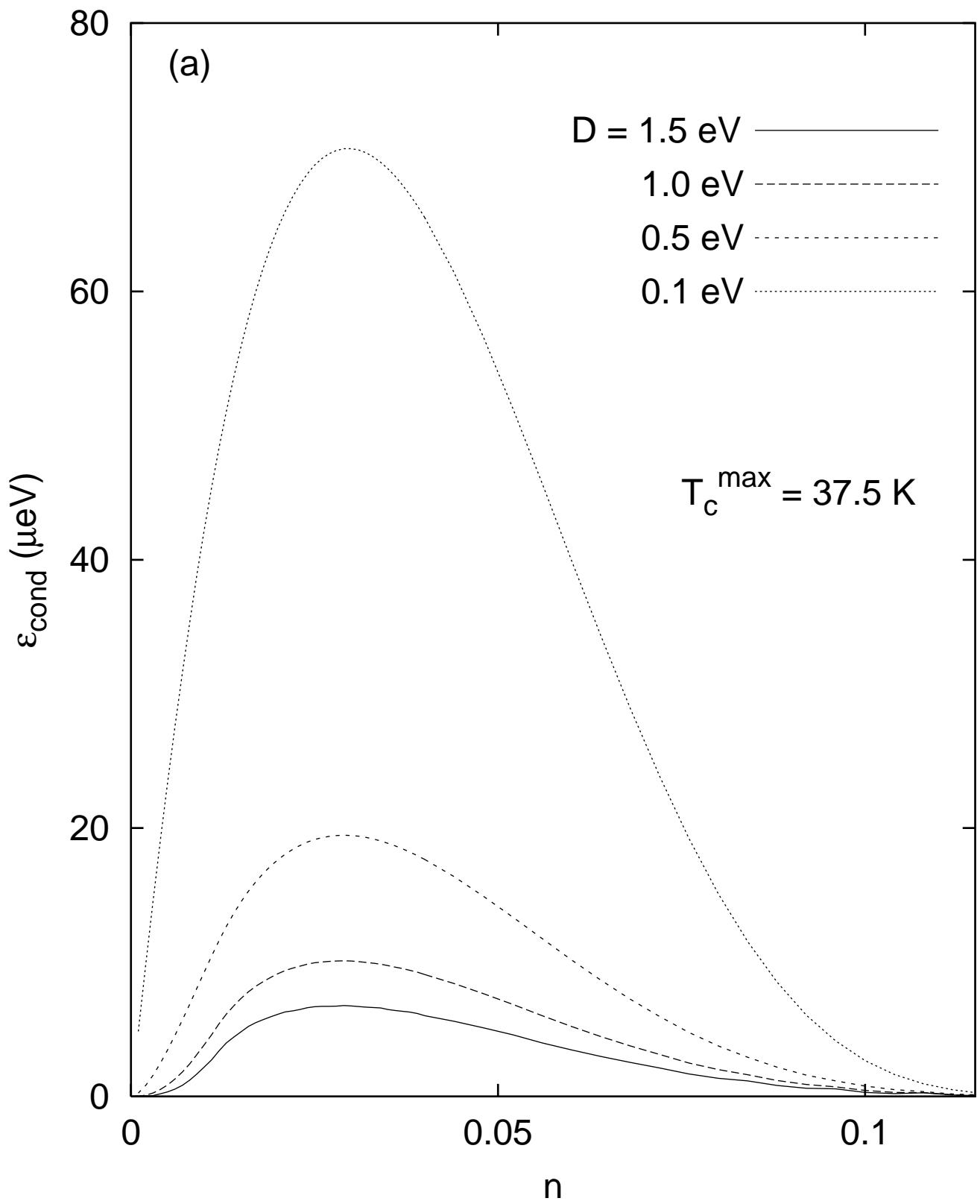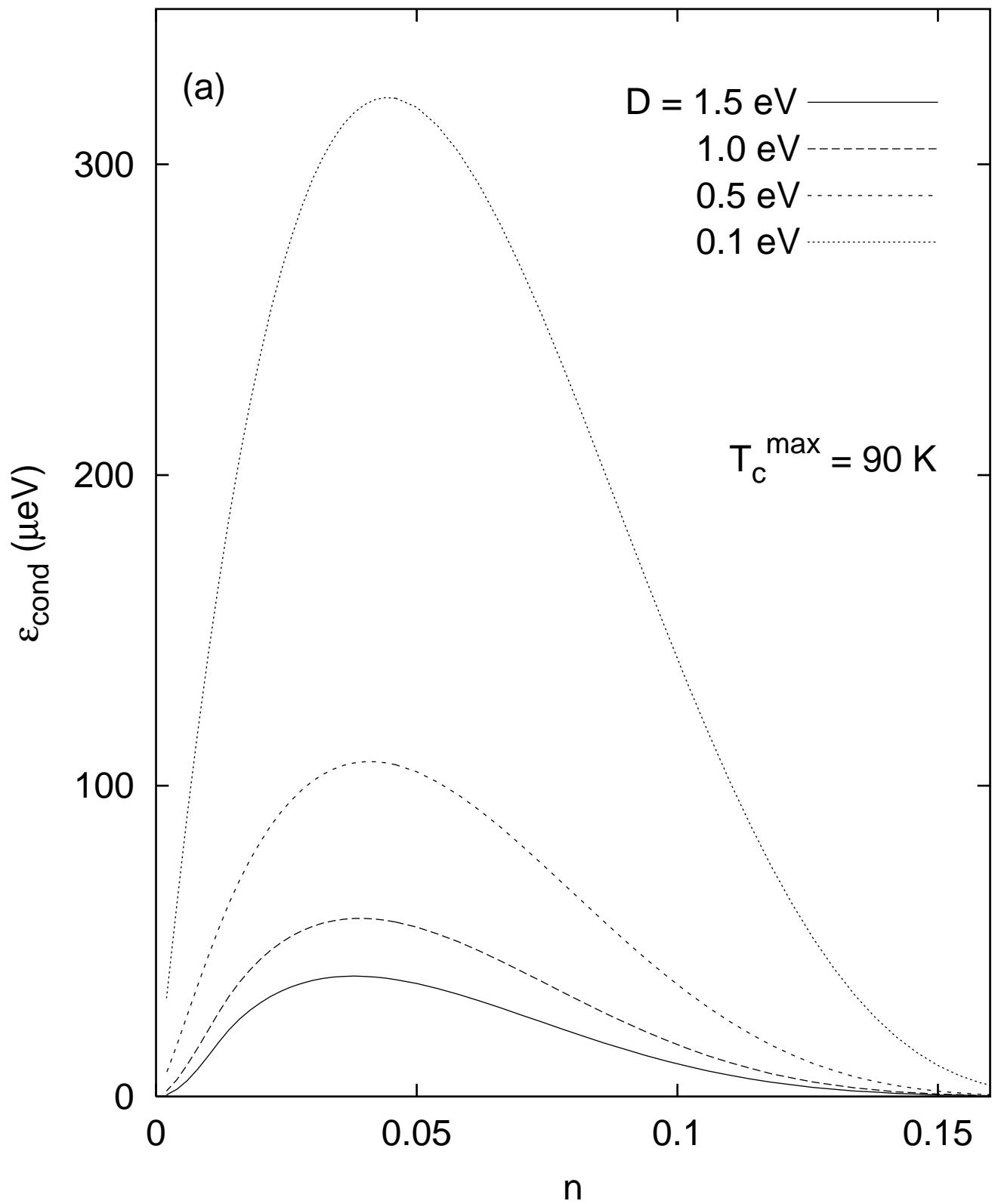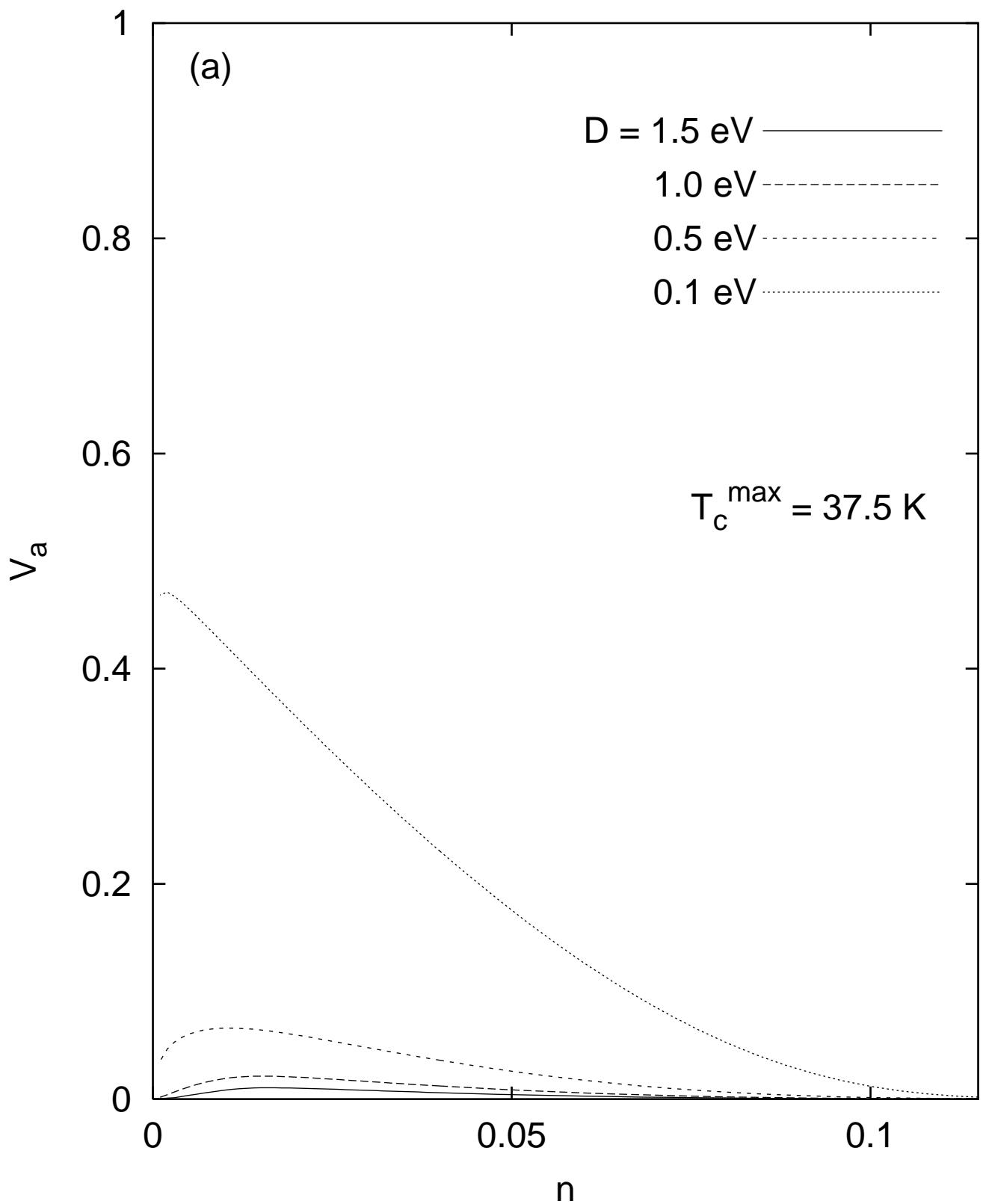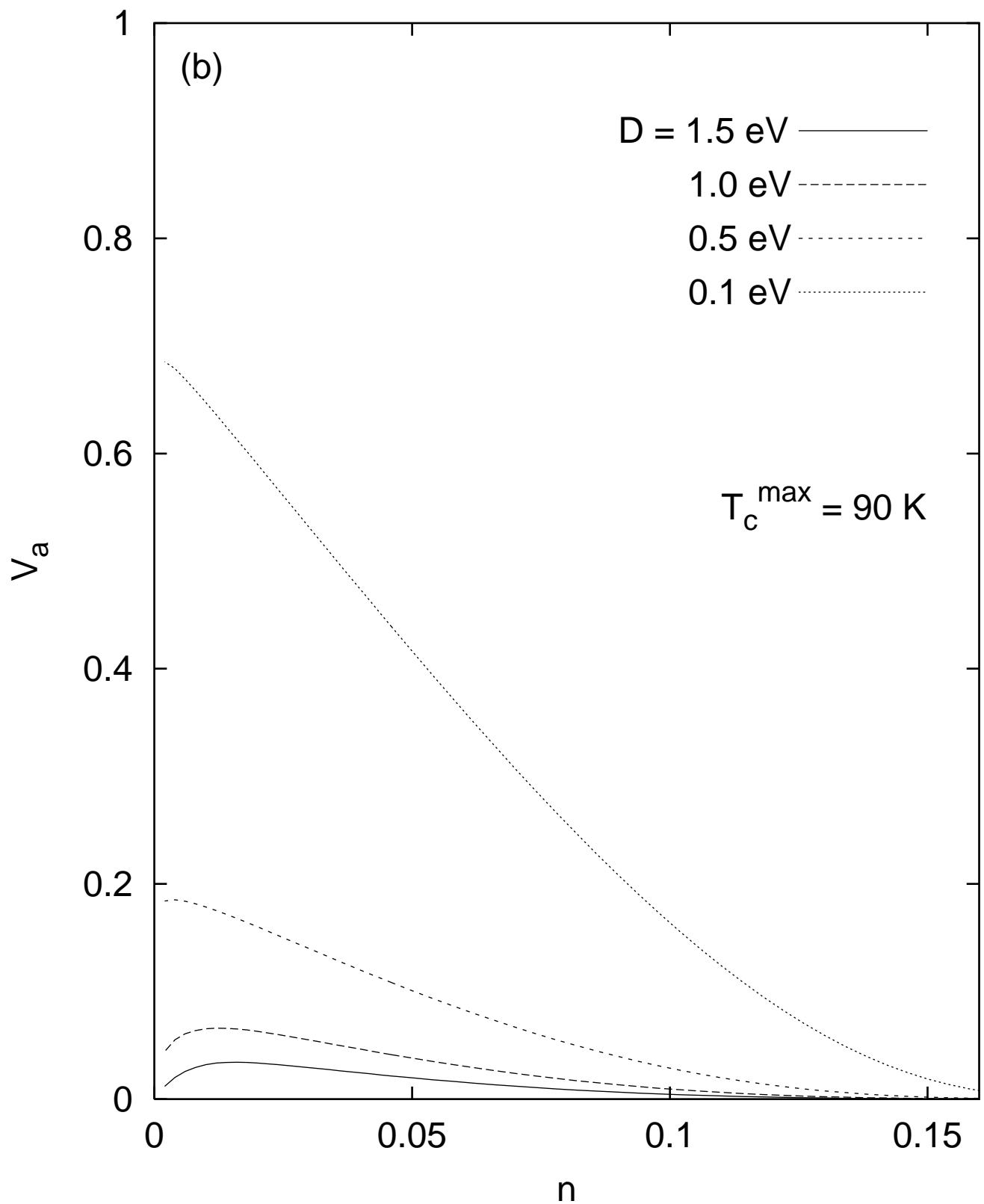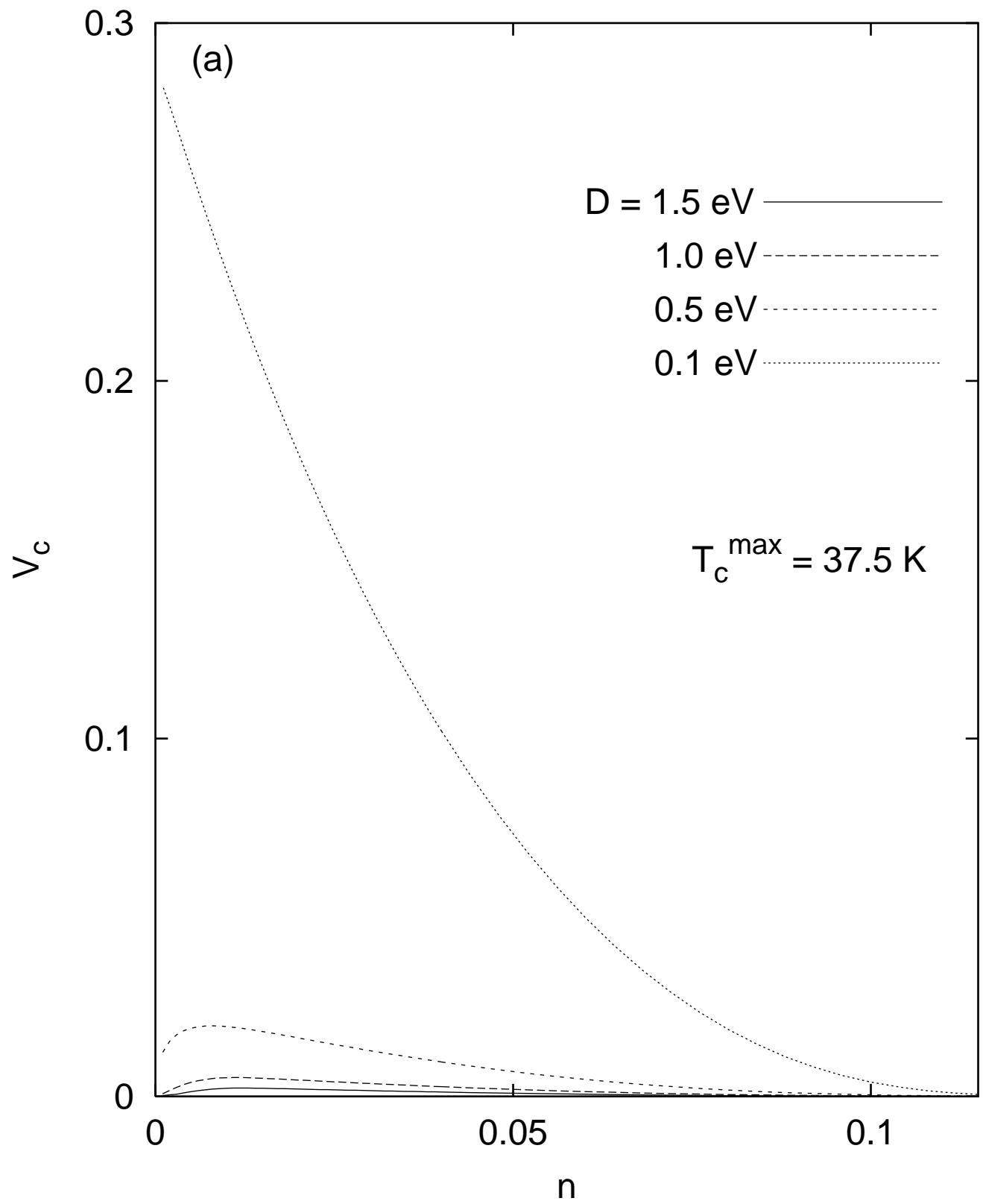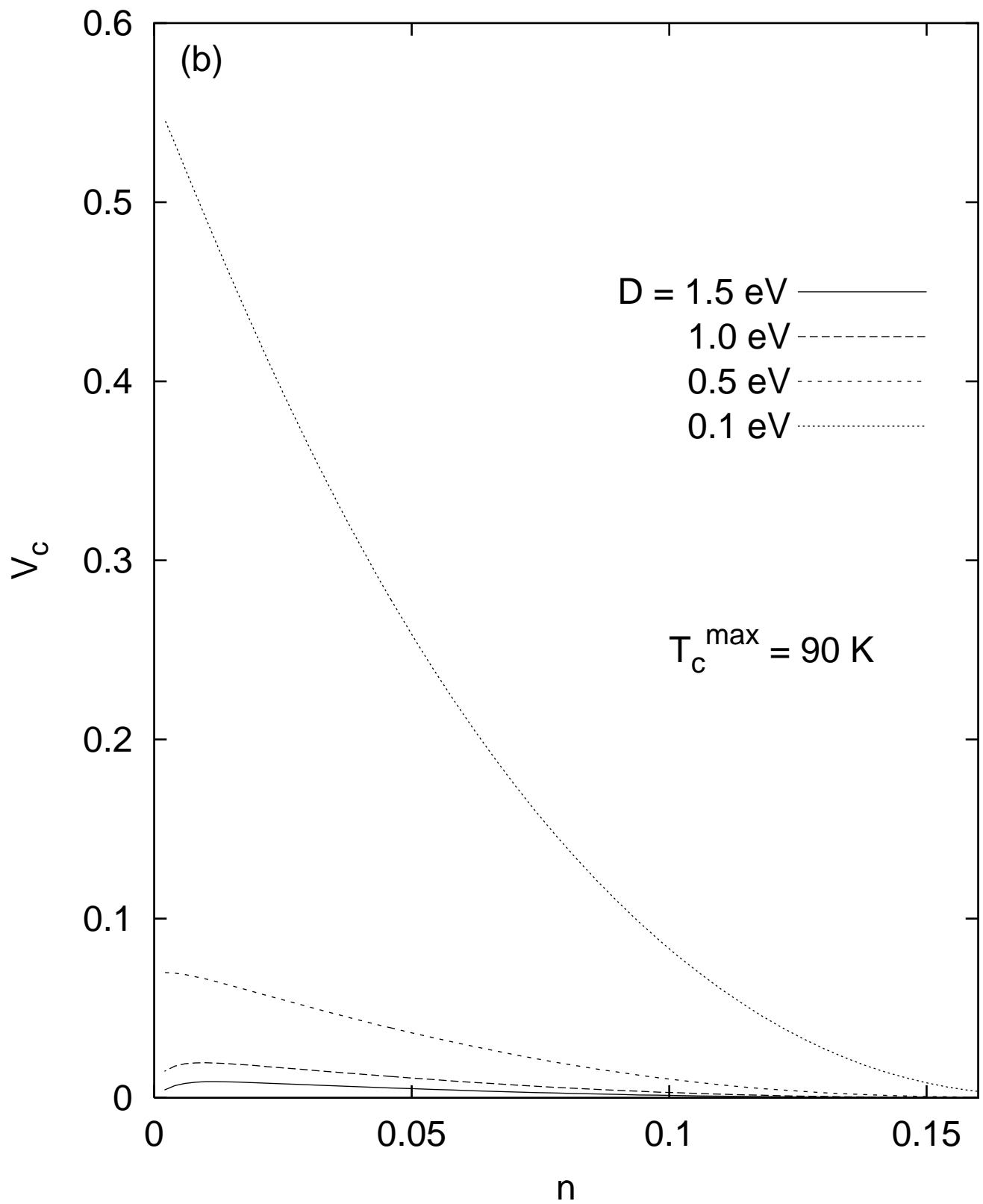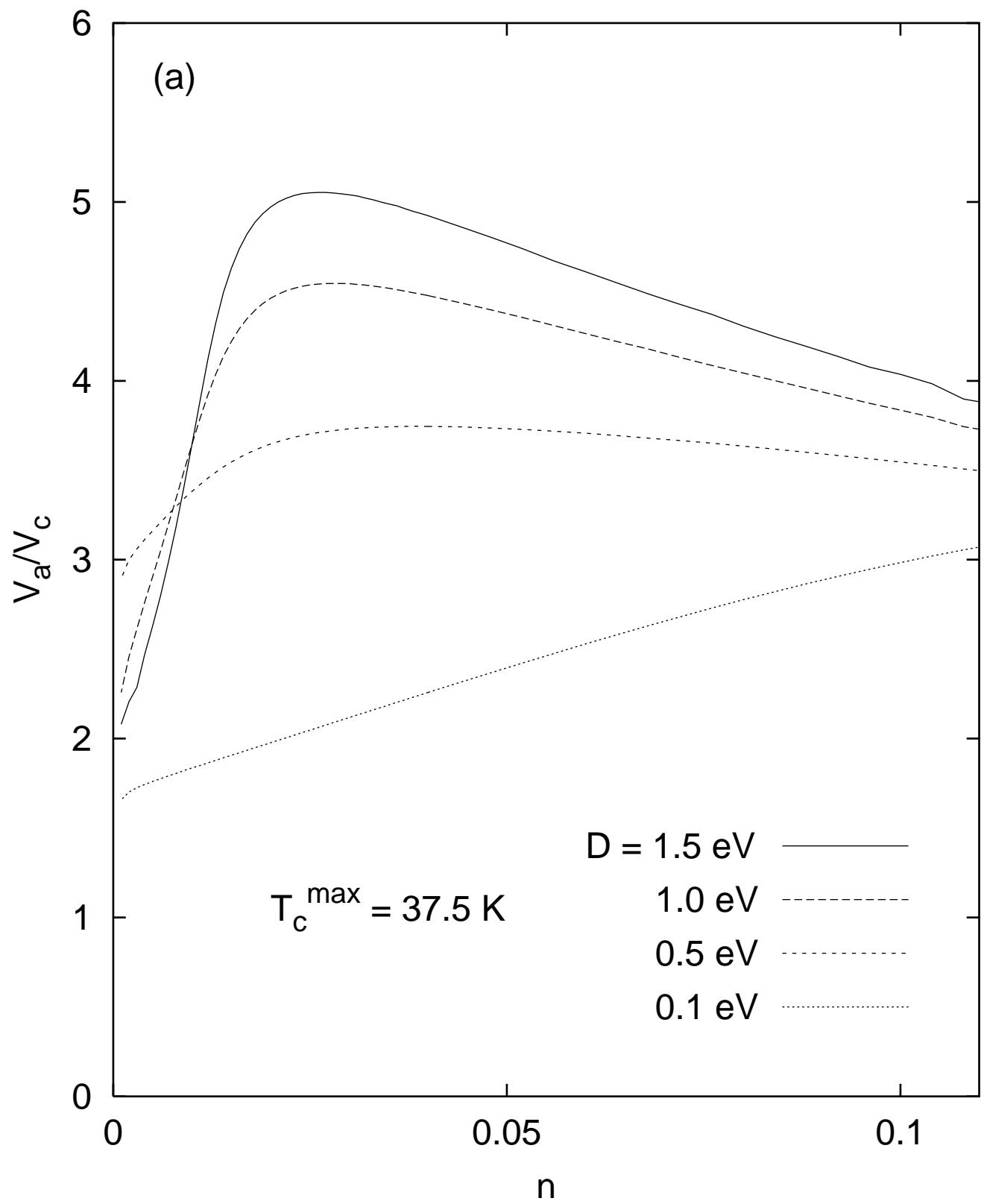
fig6b
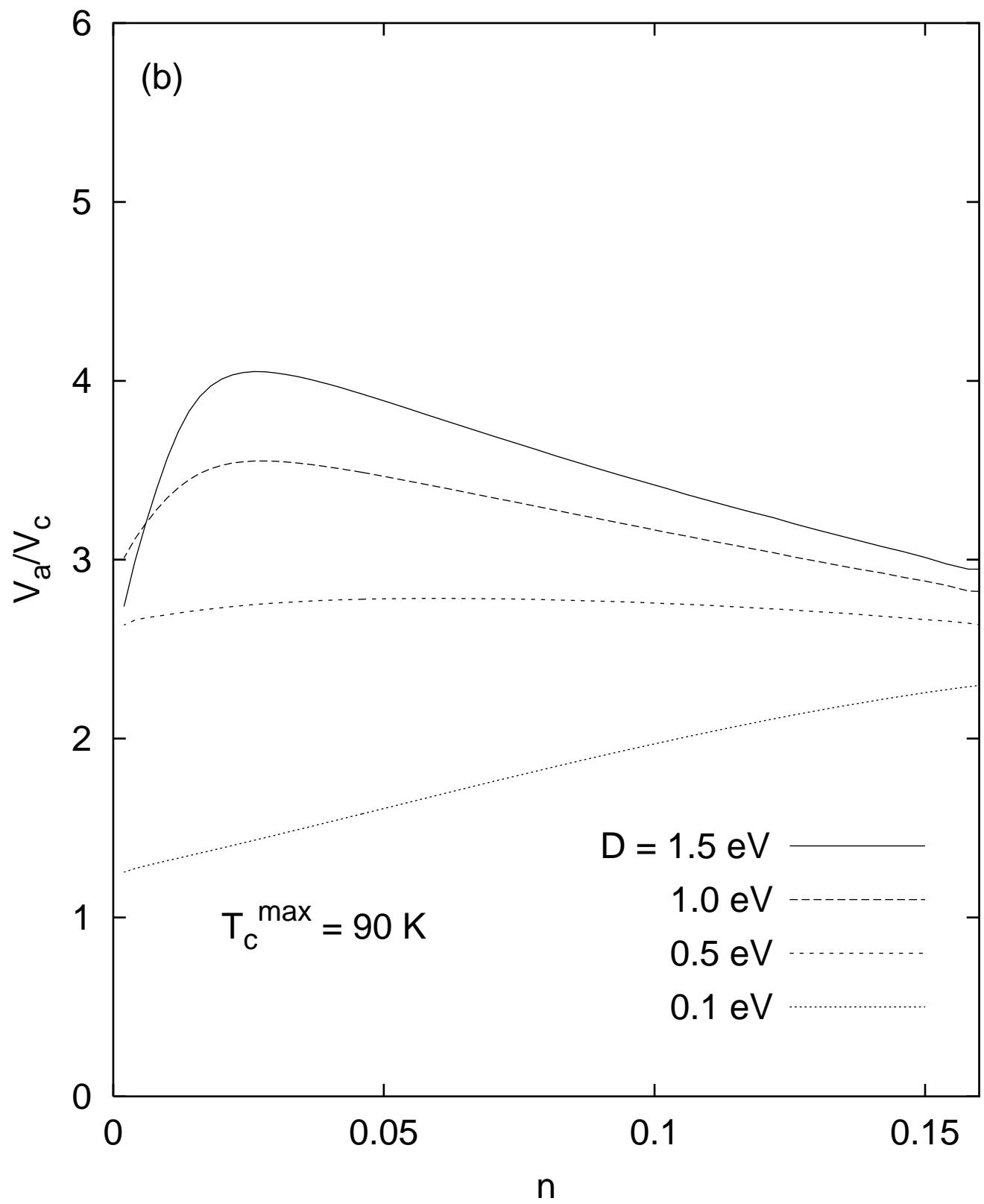
fig7a
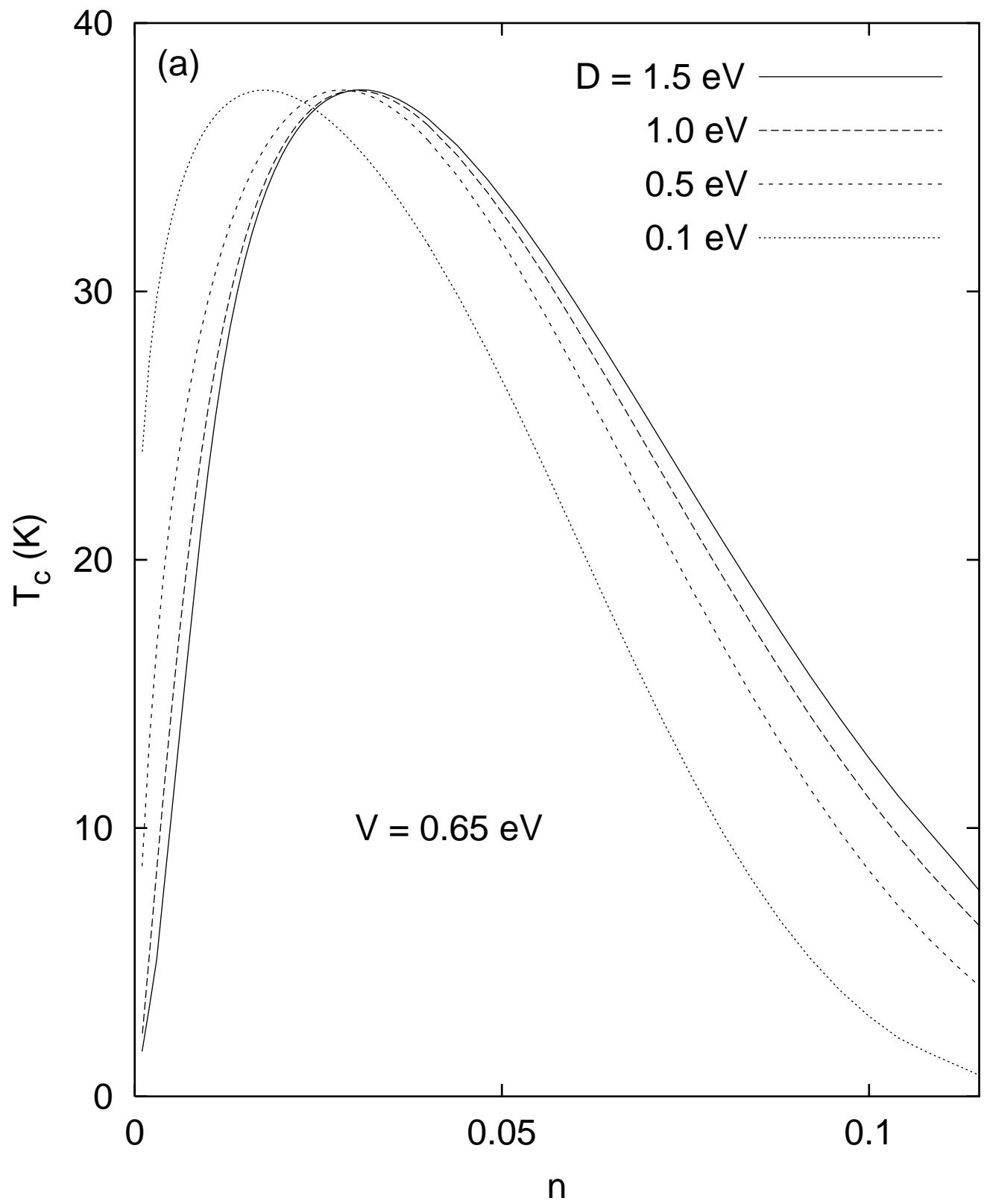
fig7b
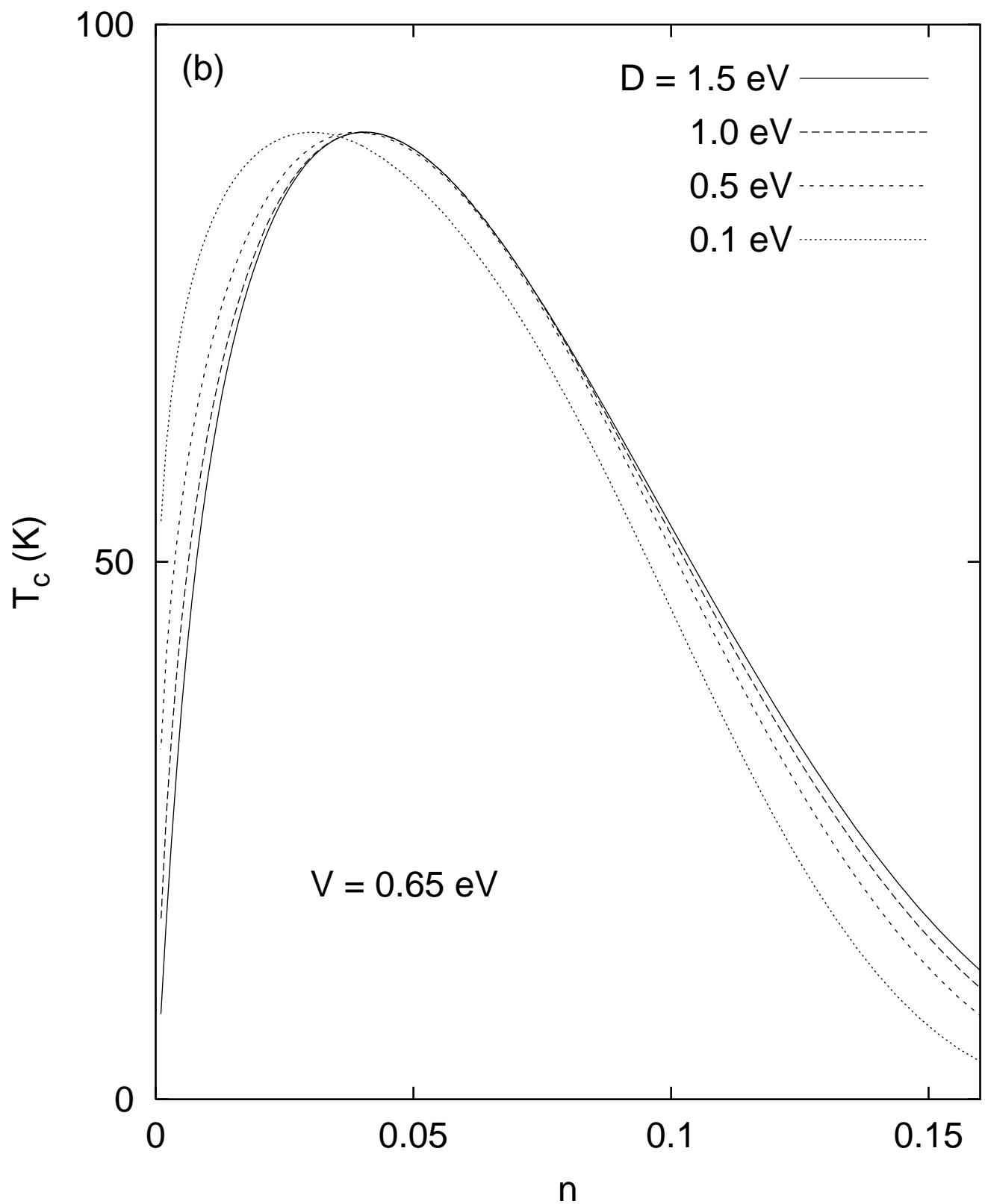
fig8a
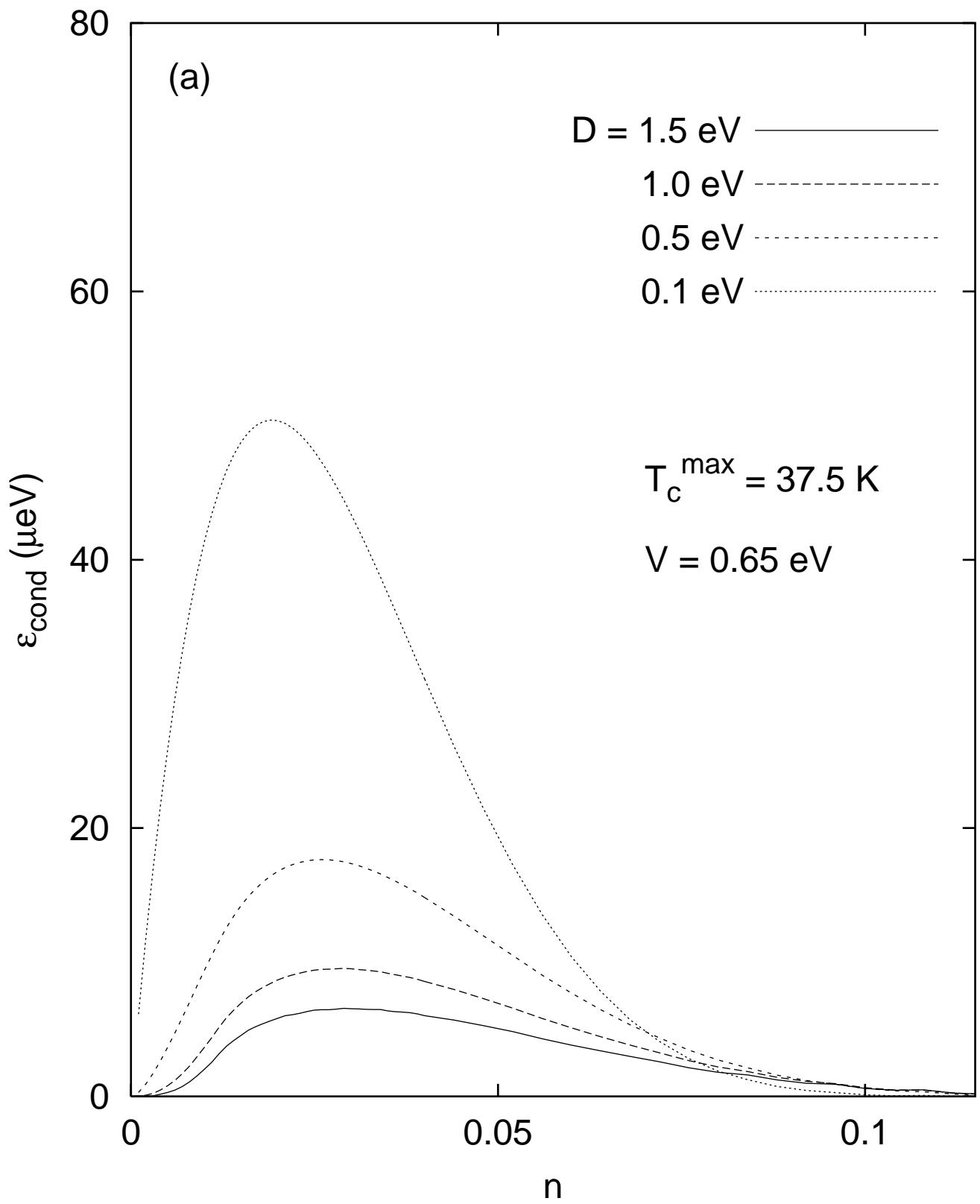
fig8b
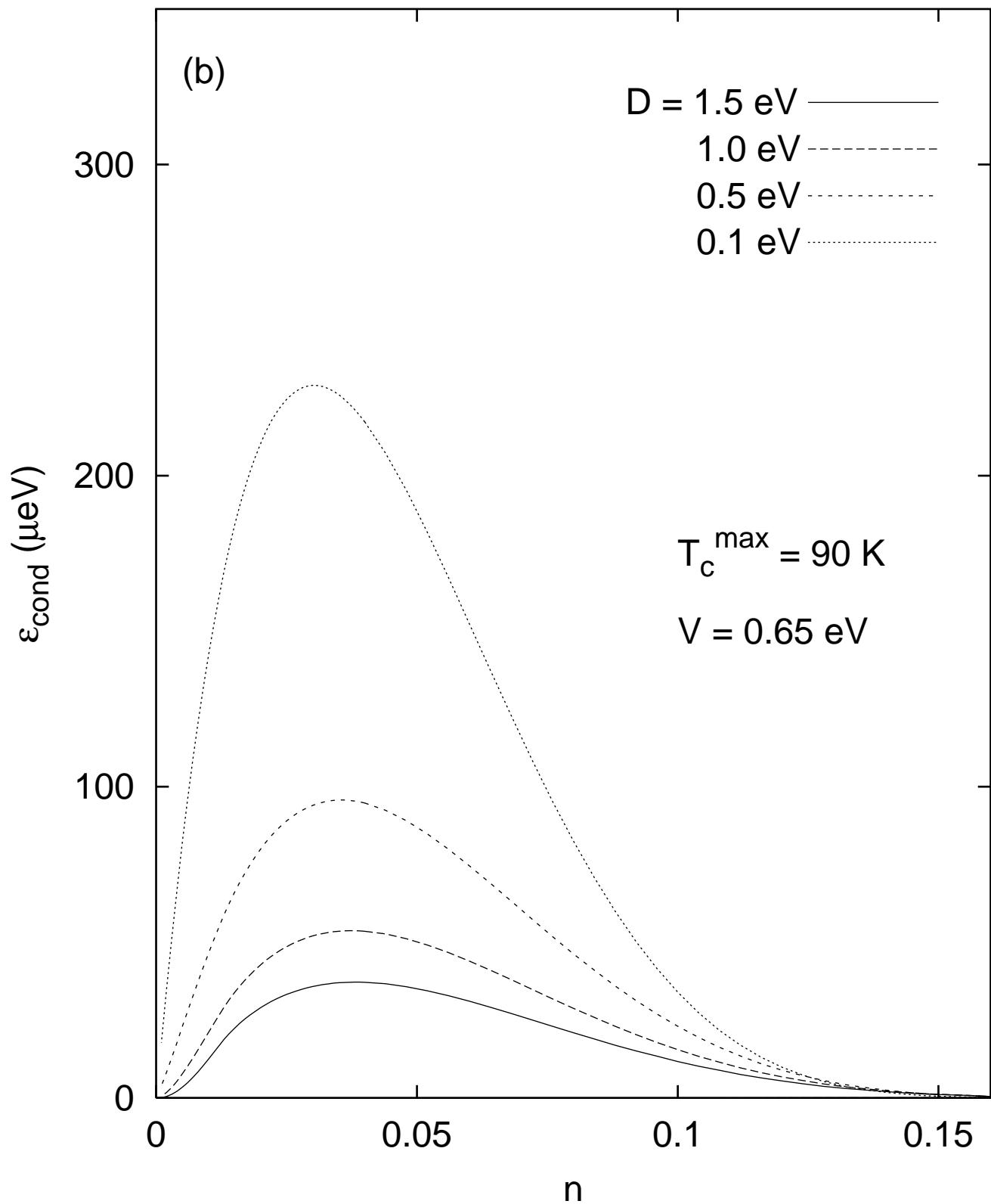
fig9a
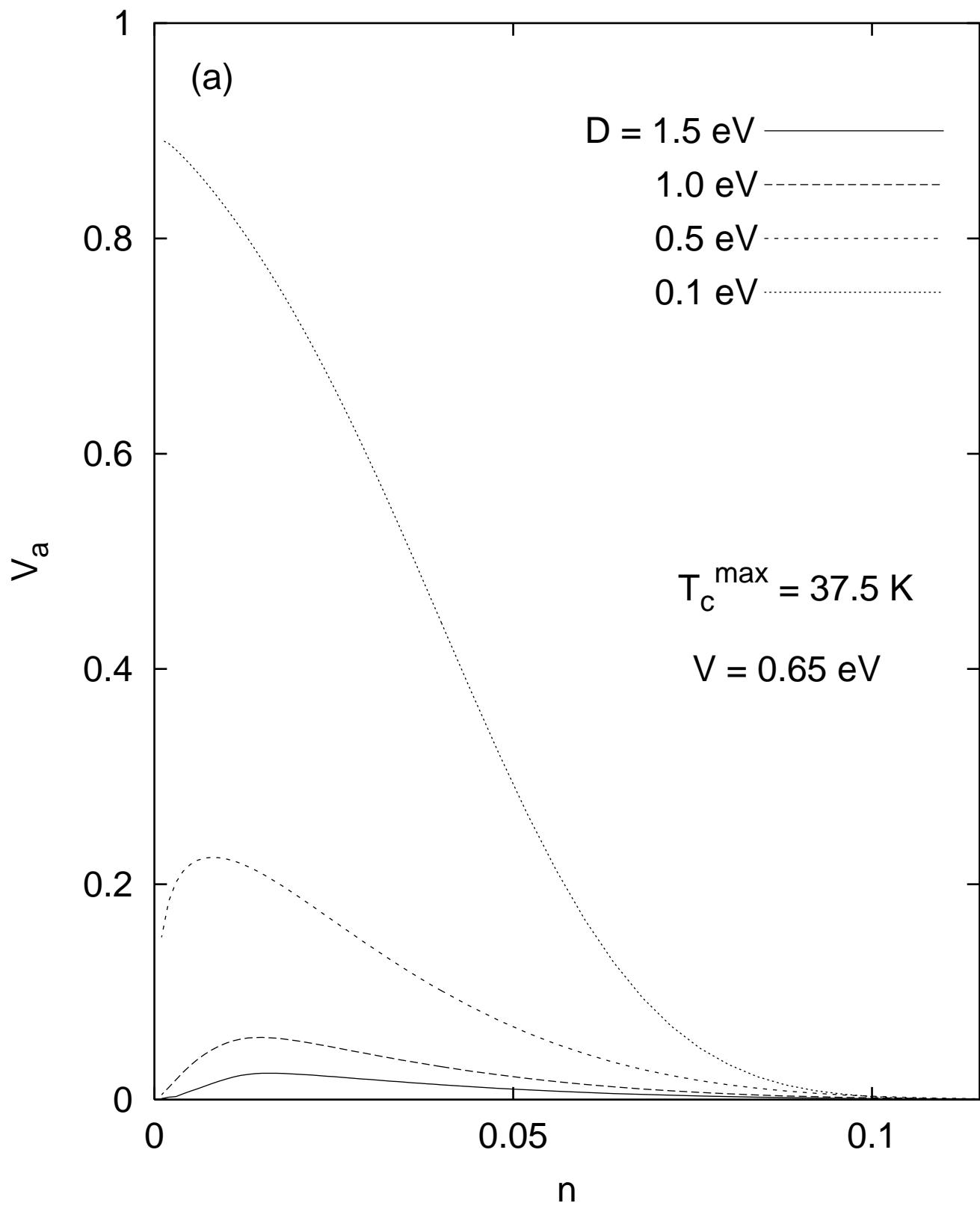
fig9b
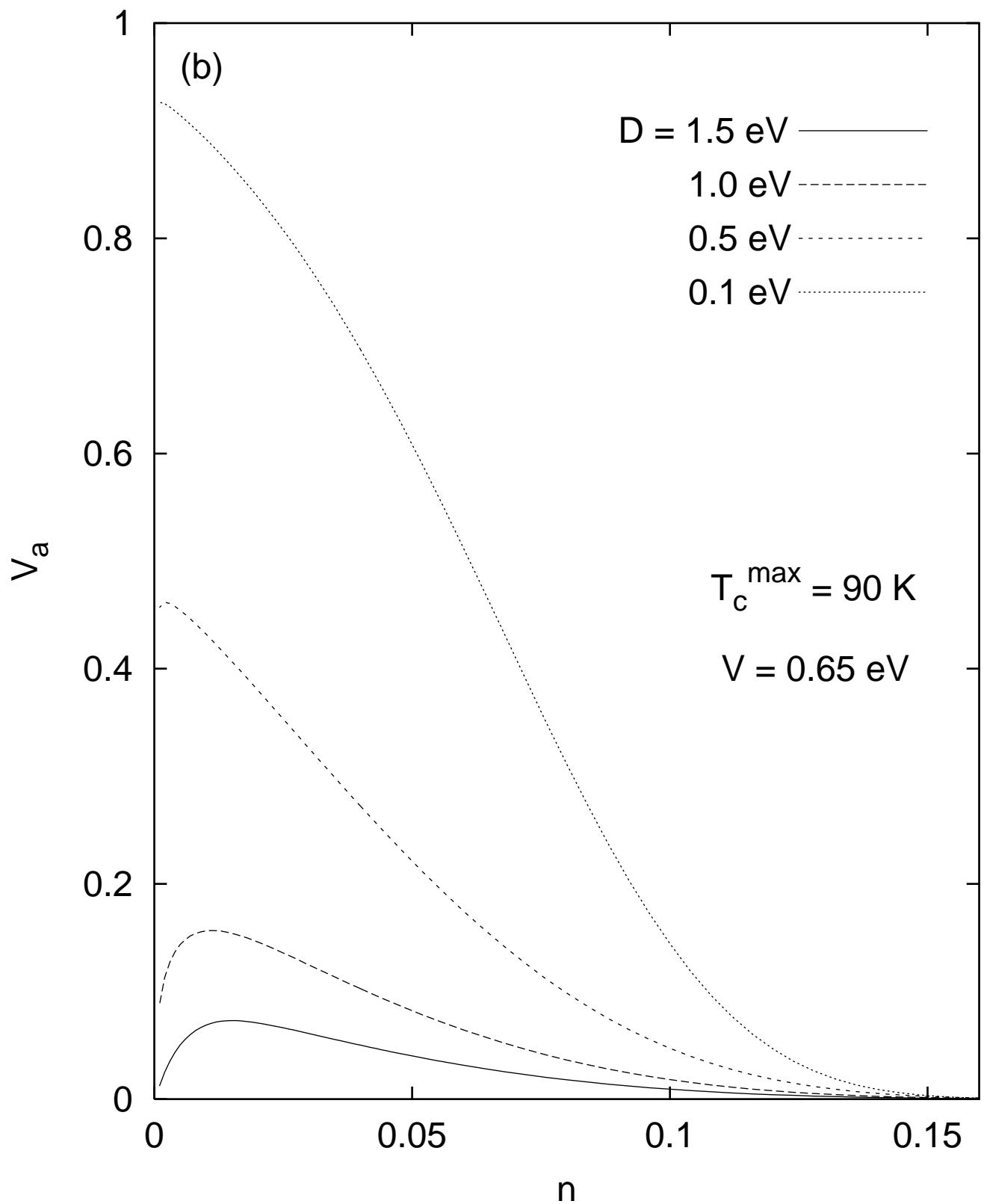
fig10a
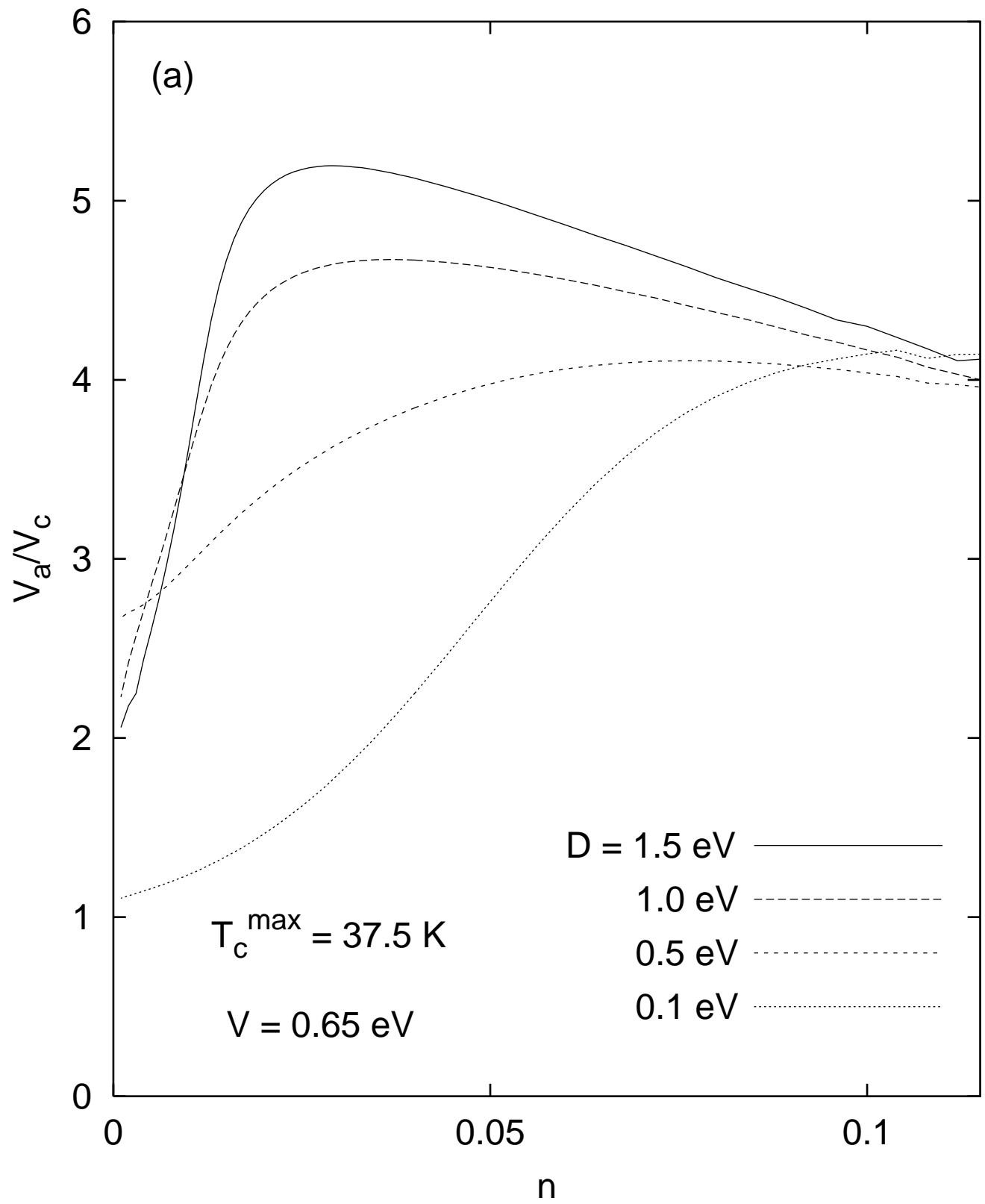
fig10b
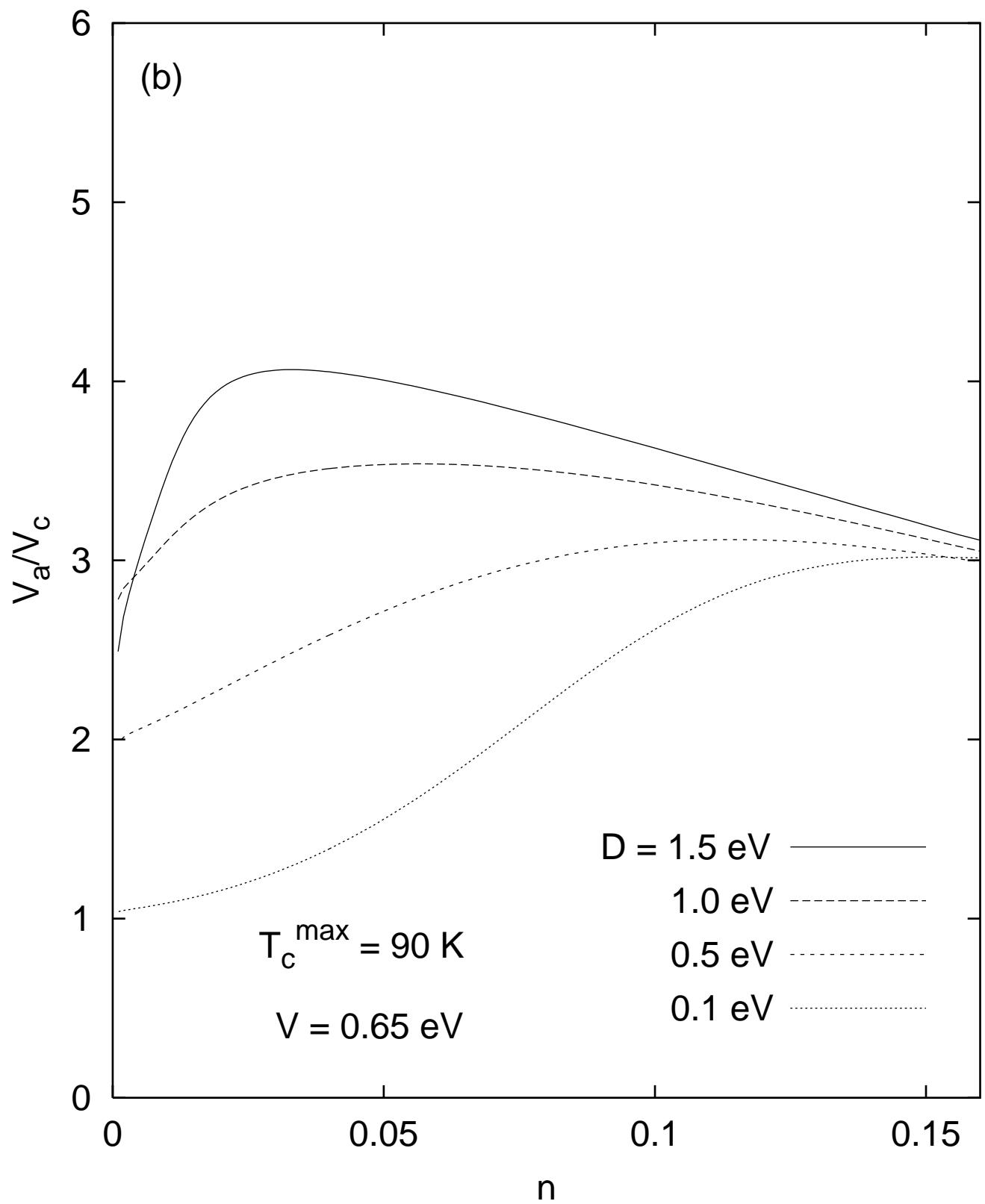
fig11a
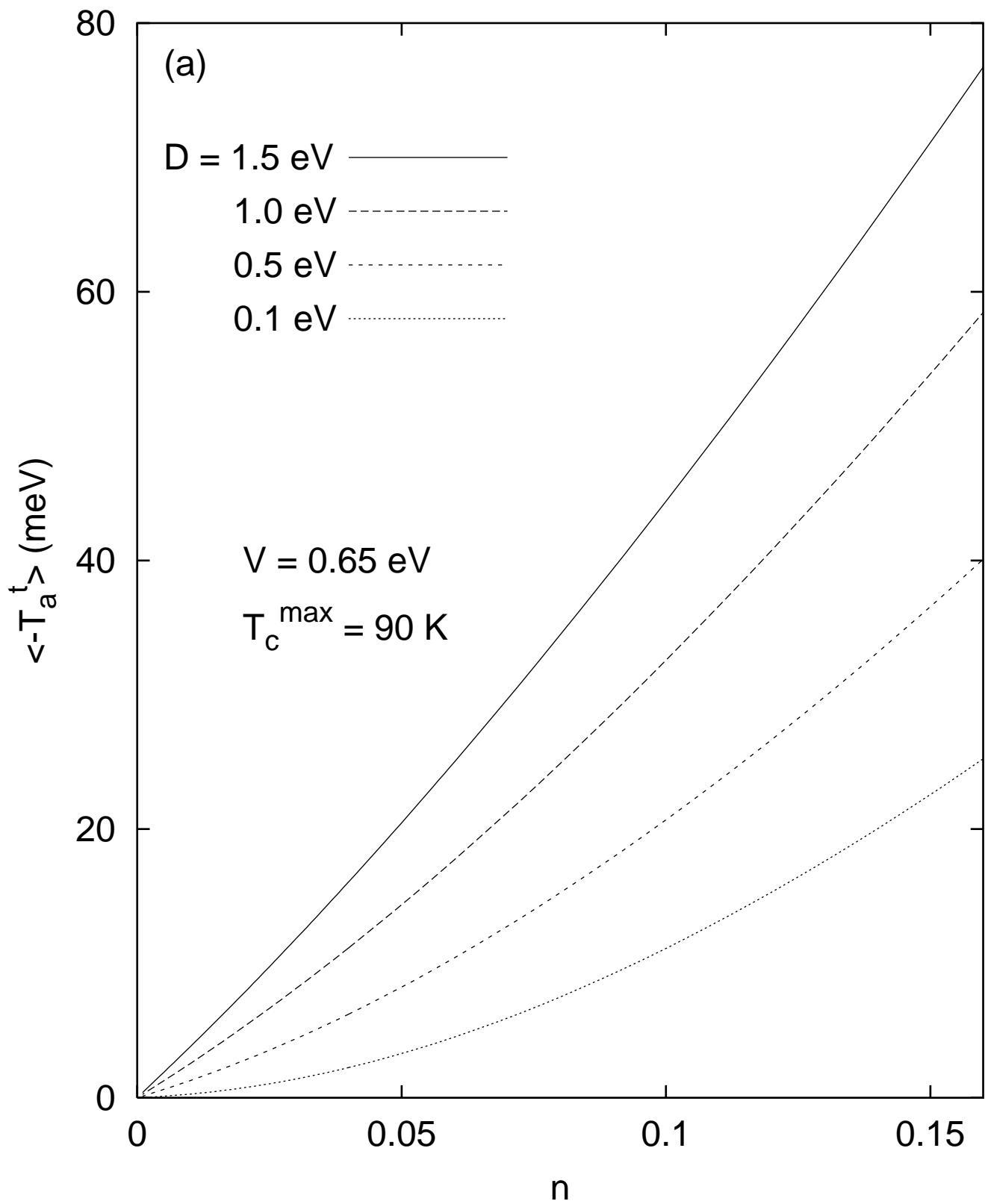
fig11b

fig11c

fig12a

fig12b

(b)

V = 0.65 eV

T_c^{max} = 90 K

D = 1.5 eV ———
1.0 eV – – –
0.5 eV - - -
0.1 eV ·······

$\langle -T_c^{\Delta t} \rangle$ (meV)

n
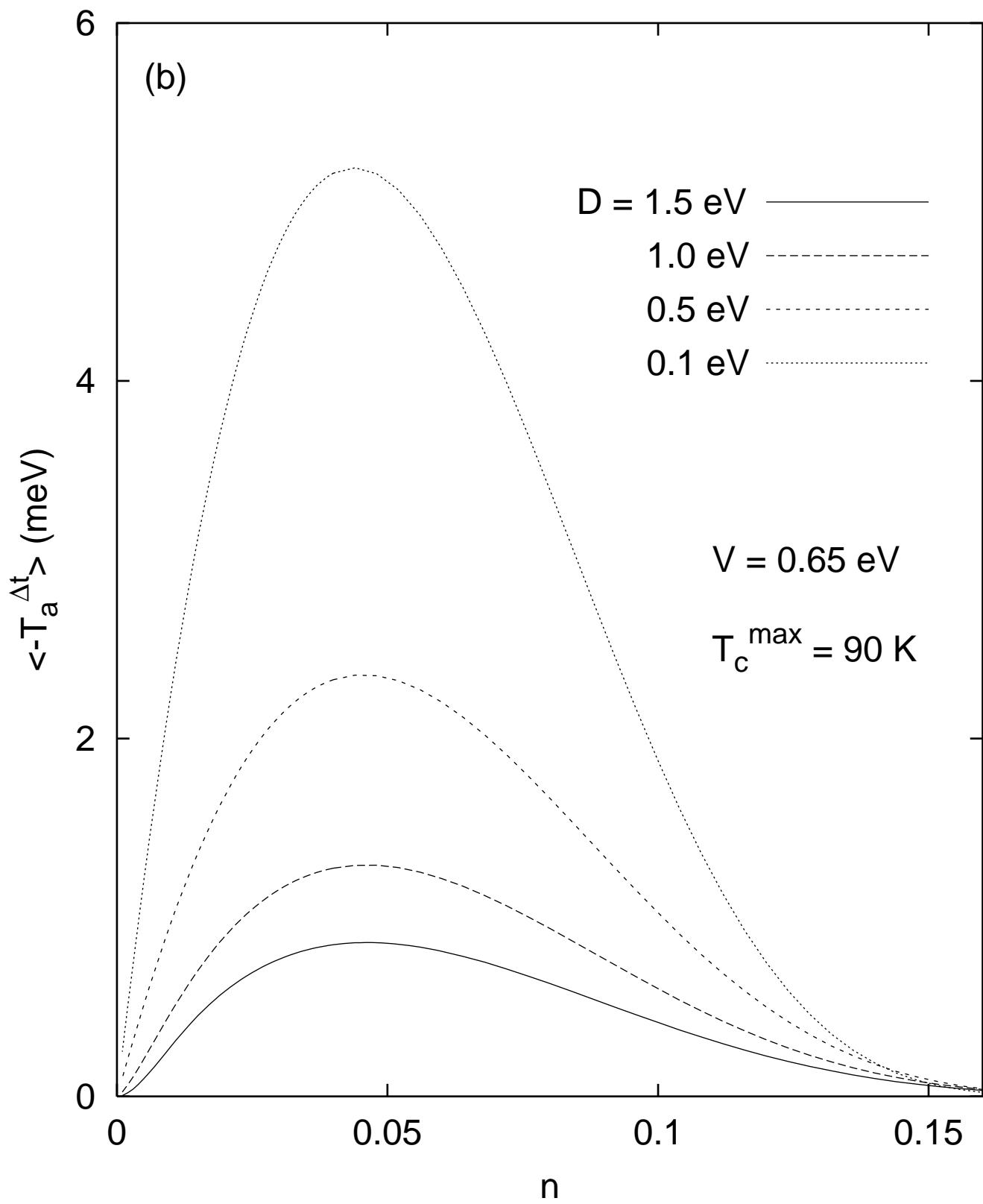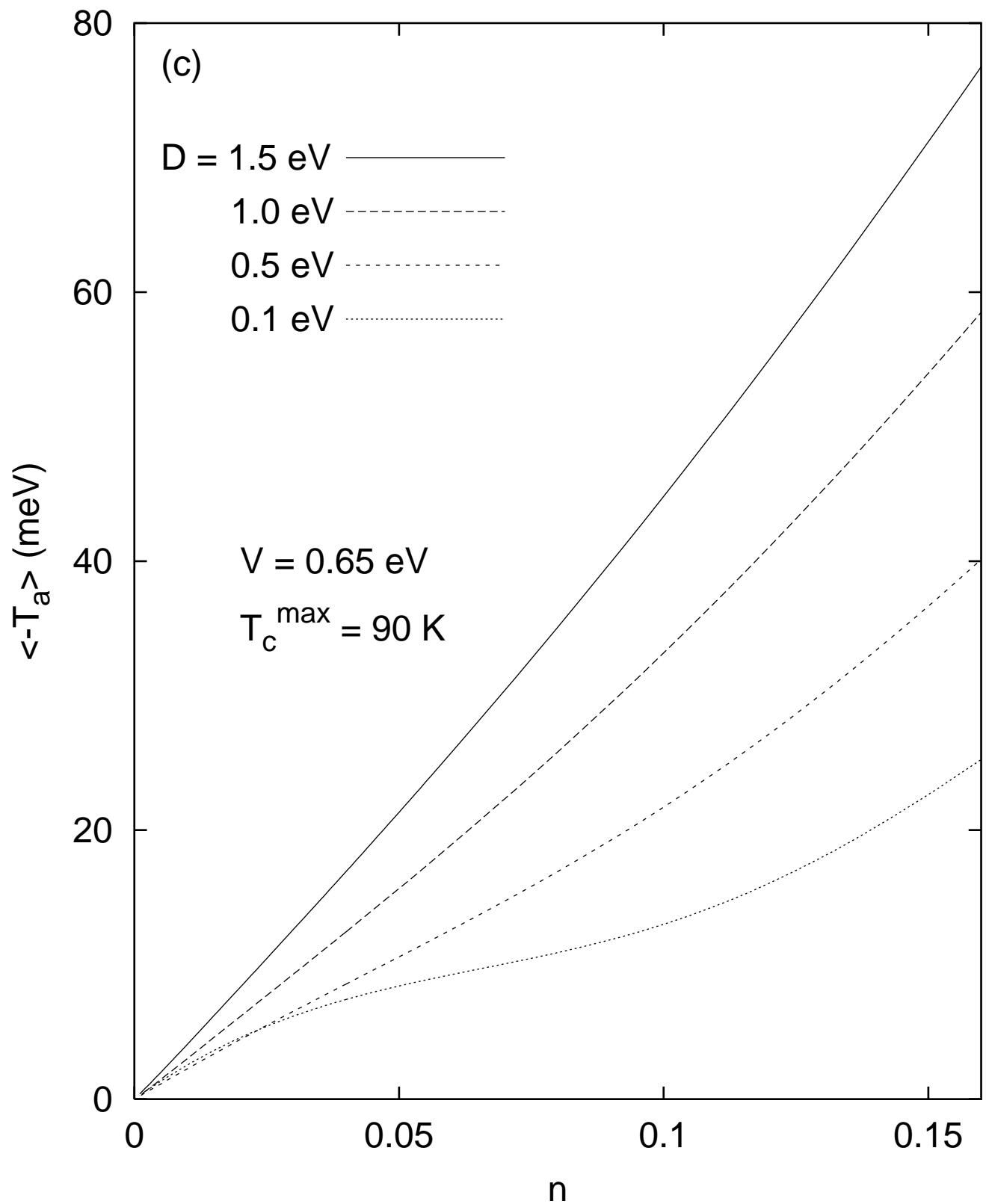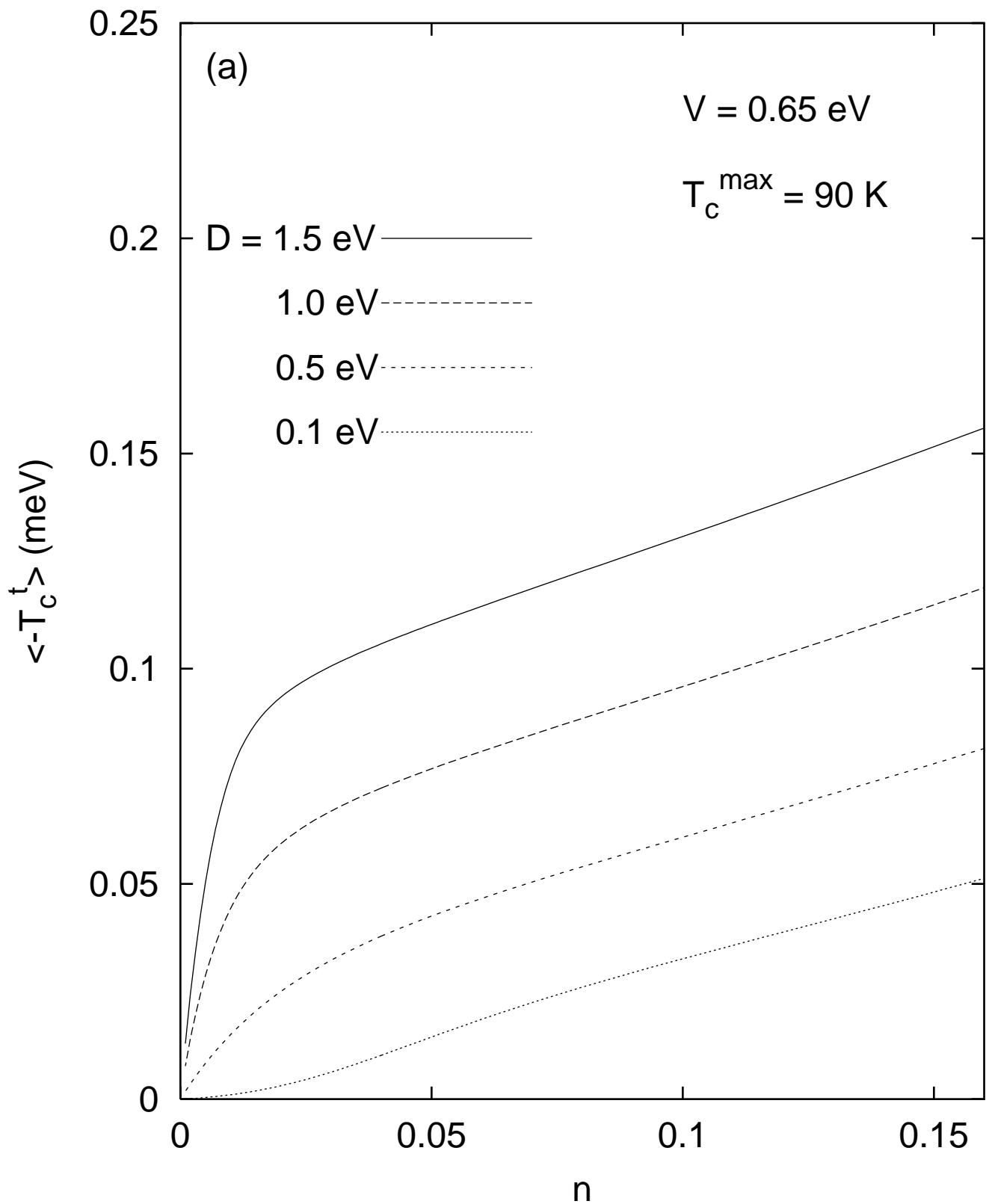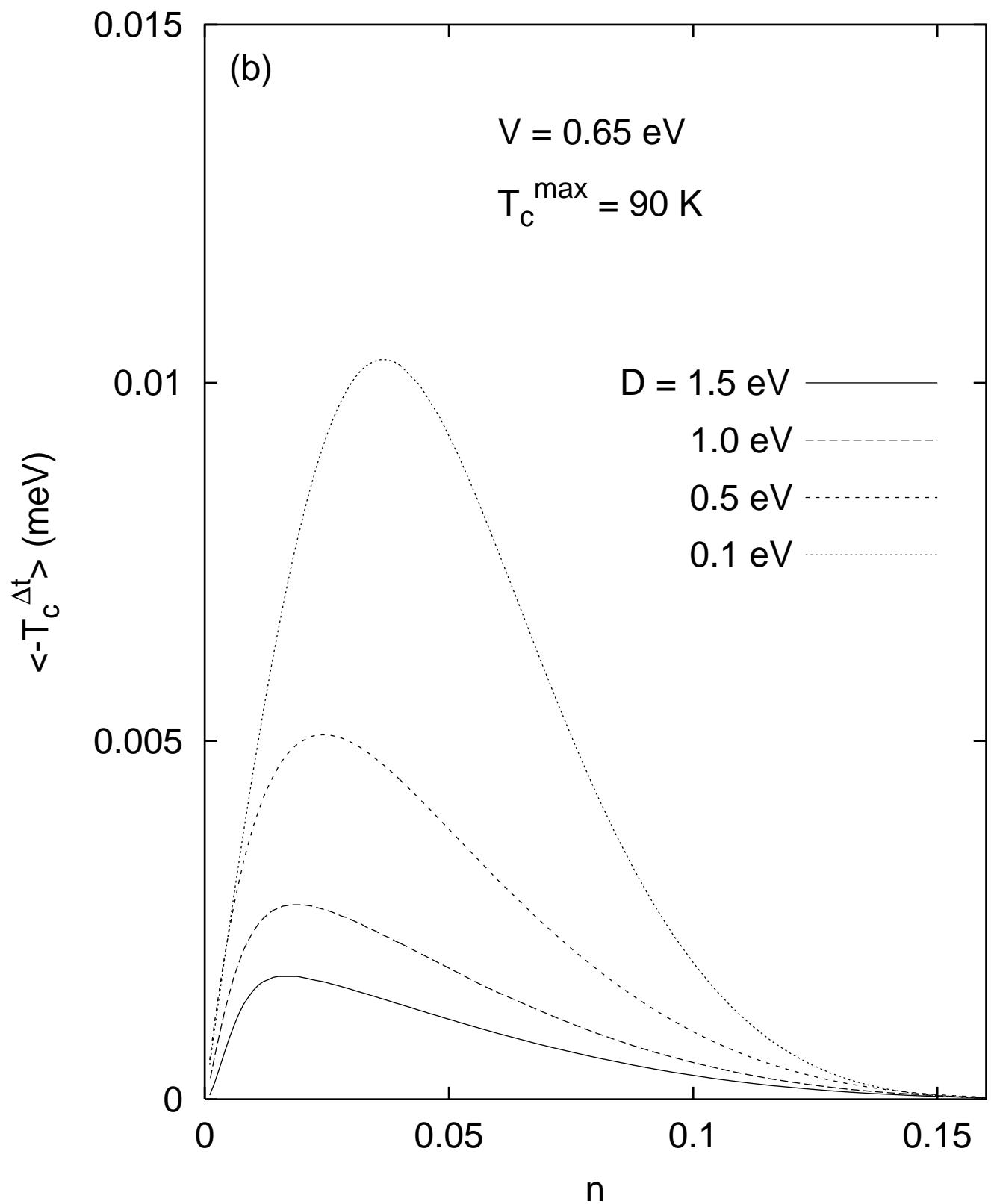
fig12c
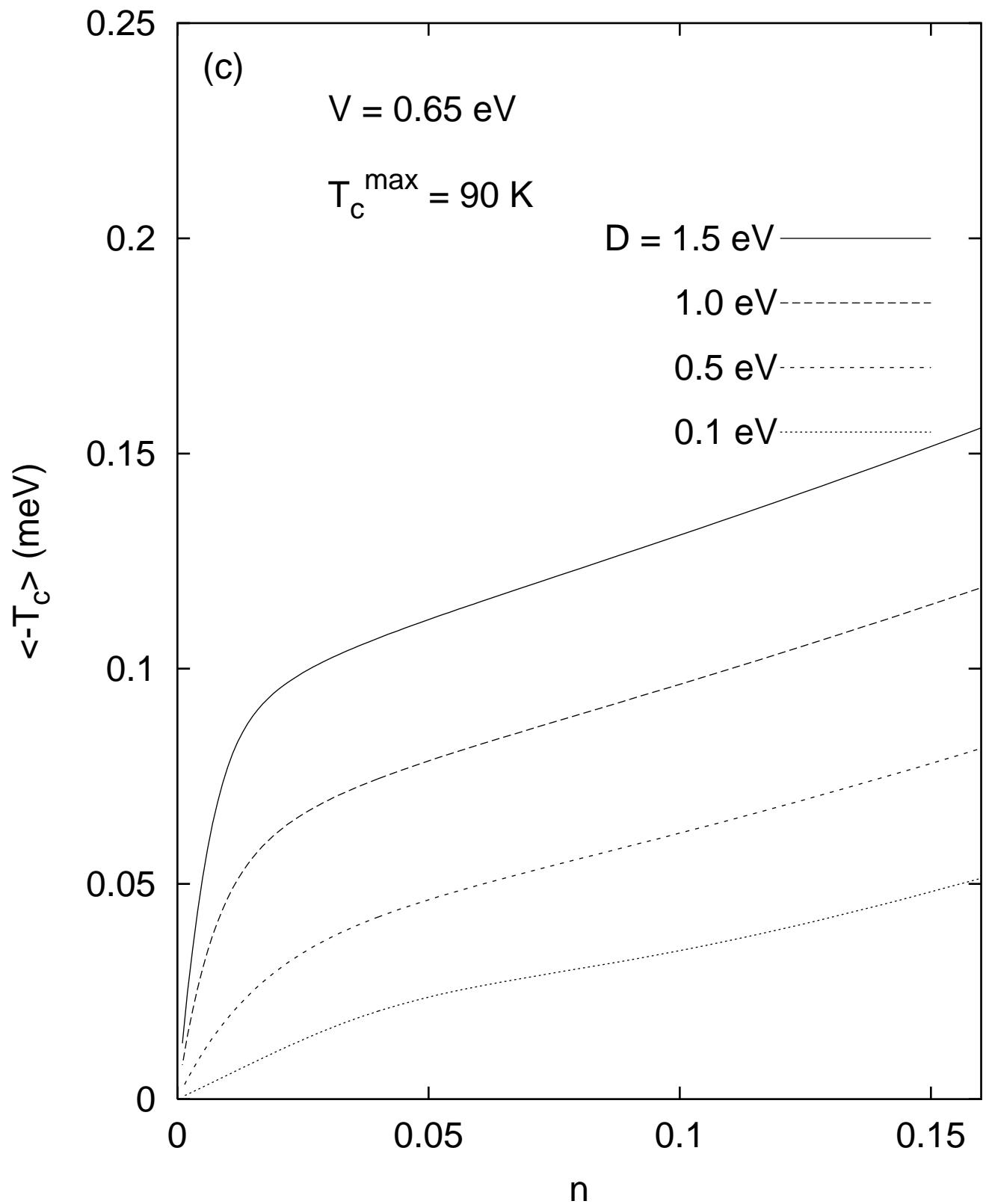
fig13a

fig13b

fig14

fig15a

(a)

D = 1.0 eV

T_c^{max} = 90 K

V = 0.65 eV

$\varepsilon_{\Delta t}$

10 X ε_{cond}

$\Delta\varepsilon_t$

ε_V

ε_U

ε (meV)

n

fig15b

fig16

fig17a

(a)

$T_c^{max} = 90$ K

$V = 0$

$V = 0.65$ eV

fig17b

(b)

$T_c^{max} = 90$ K

V = 0

V = 0.65 eV

V_c

D (eV)

fig18

fig19a

(a)

D = 0.5 eV

η = 10

V = 0

V = 0.65 eV

fig19b

fig20a

fig20b

(b)

D = 0.5 eV

T_c^{max} = 90 K

V = 0

Eq. (55b) ——

Expt. □

λ_c (A)

n
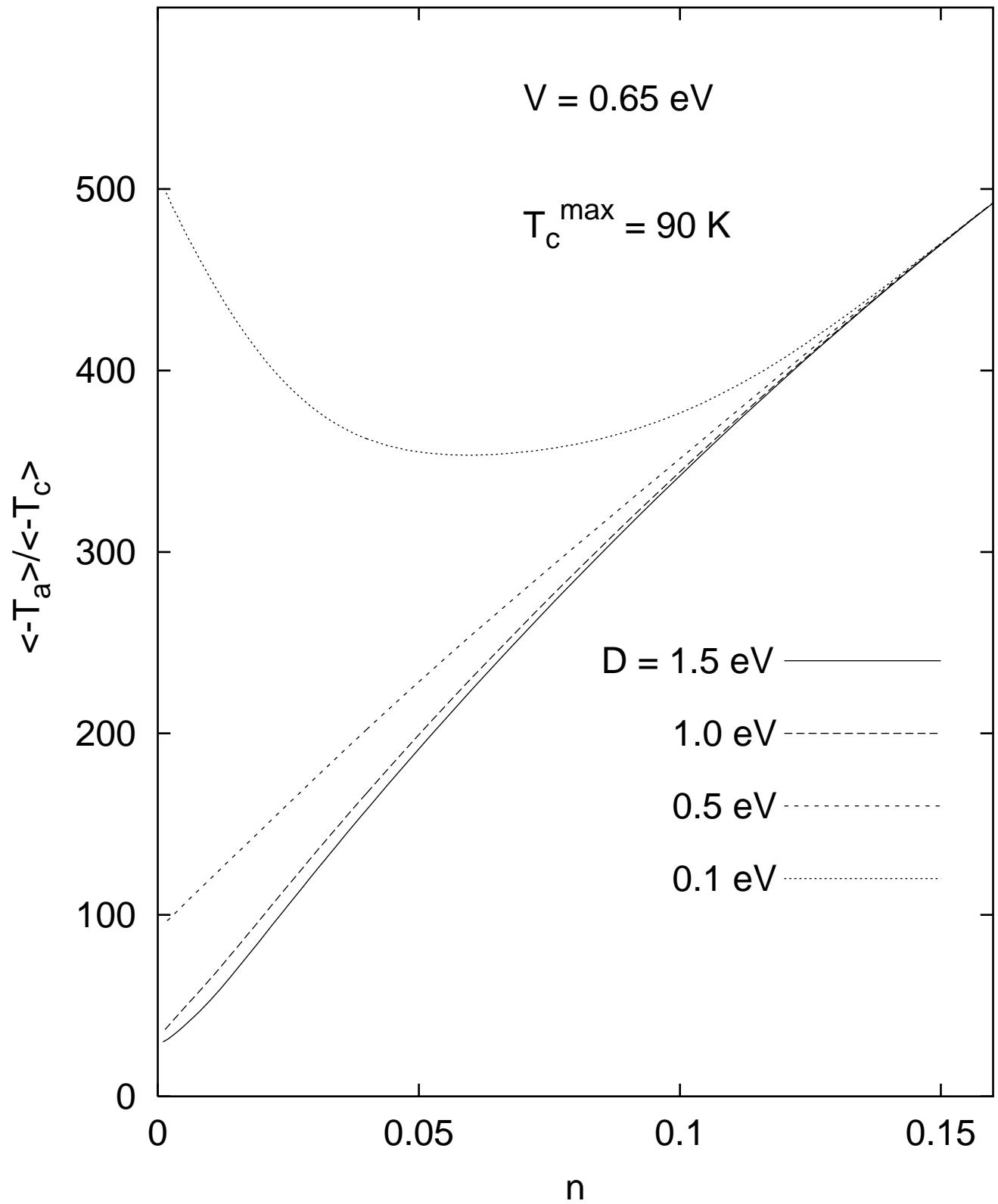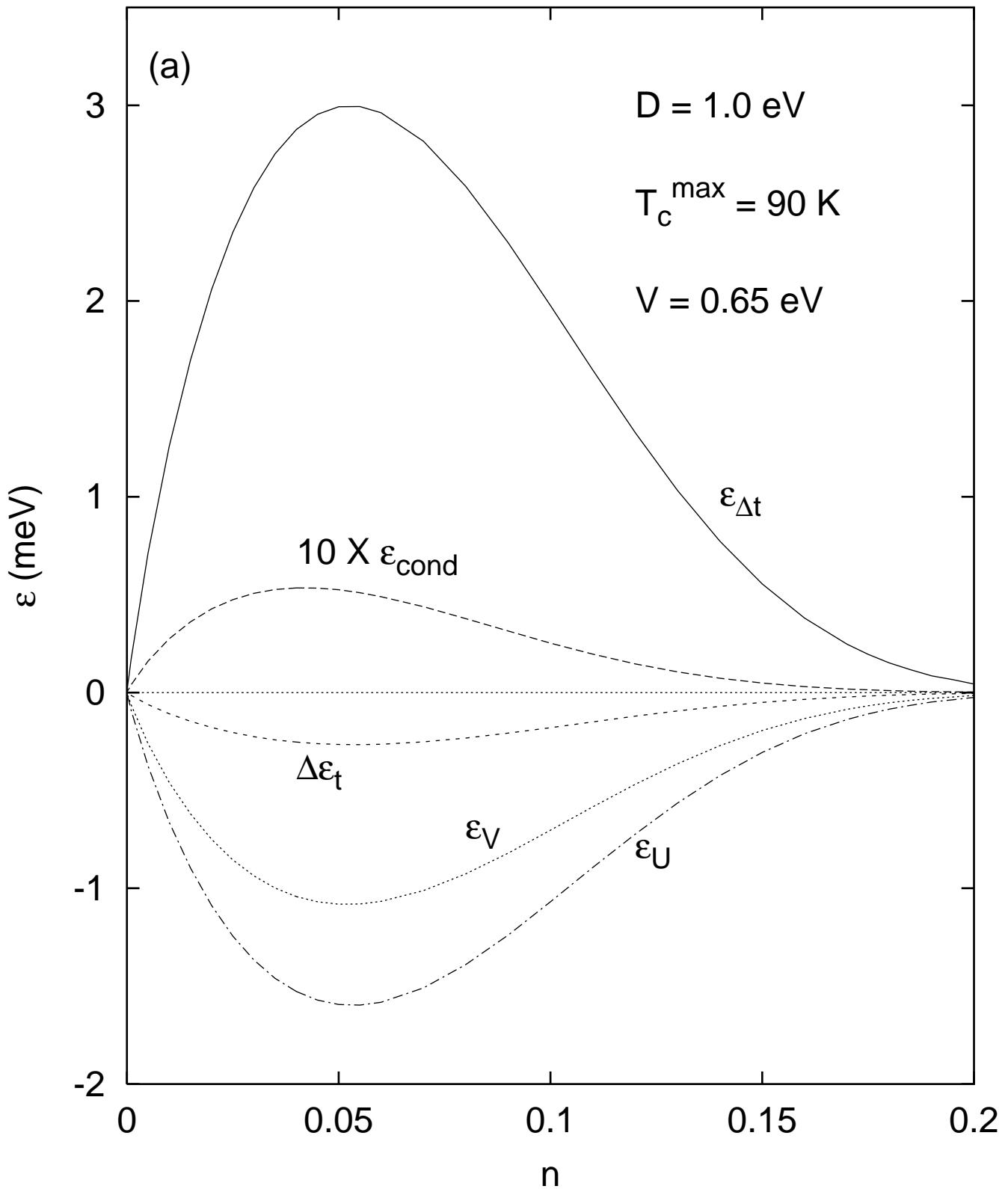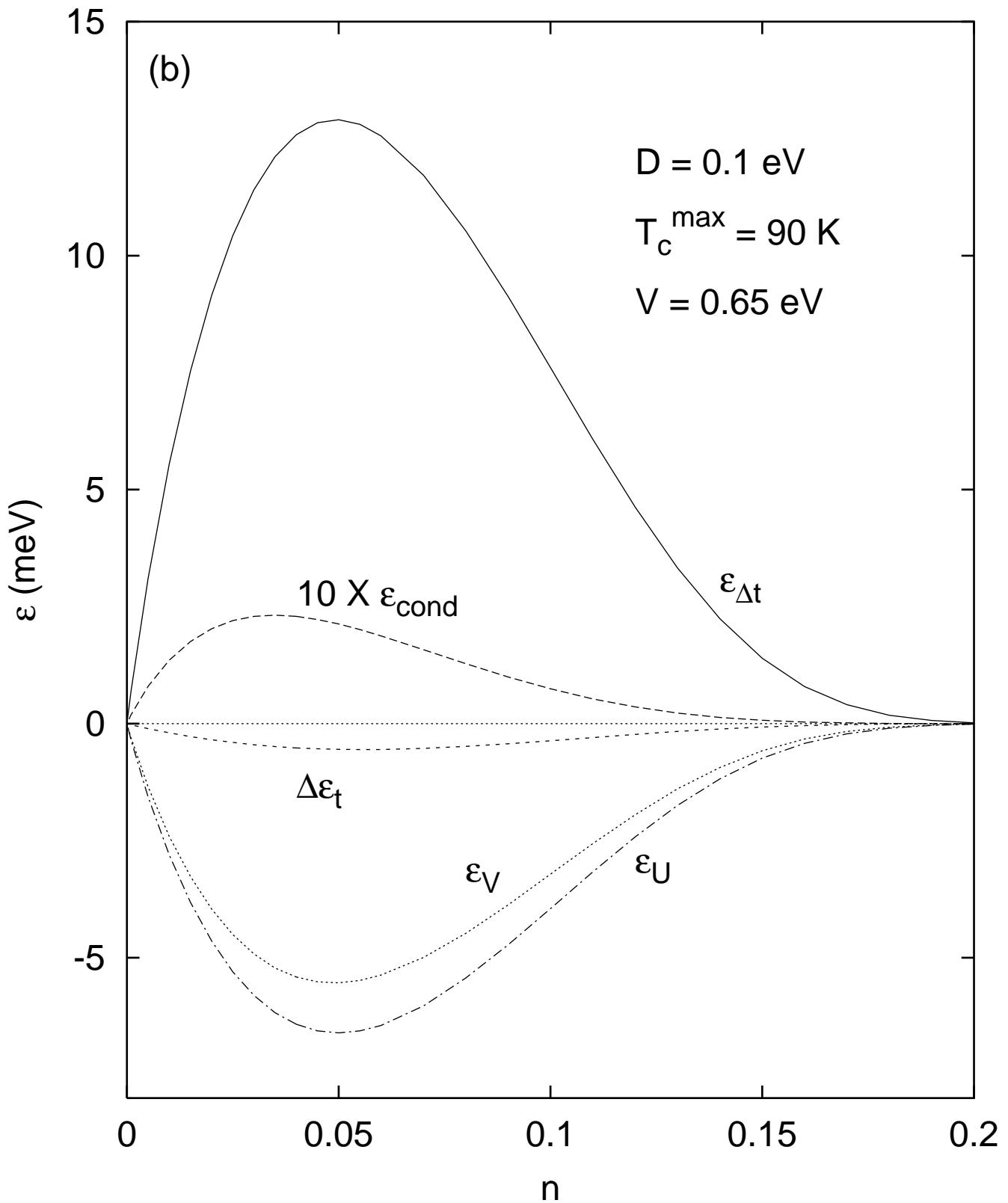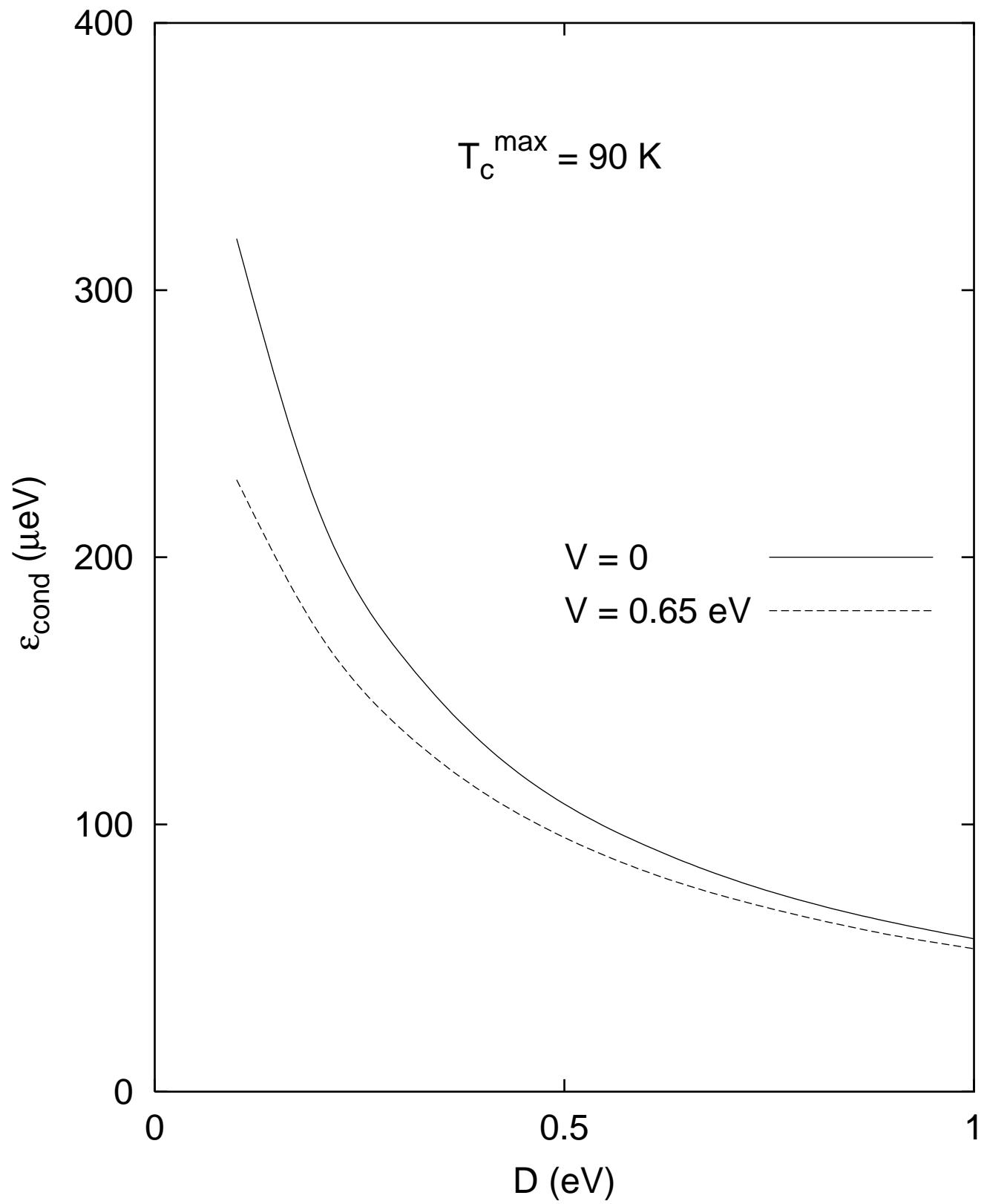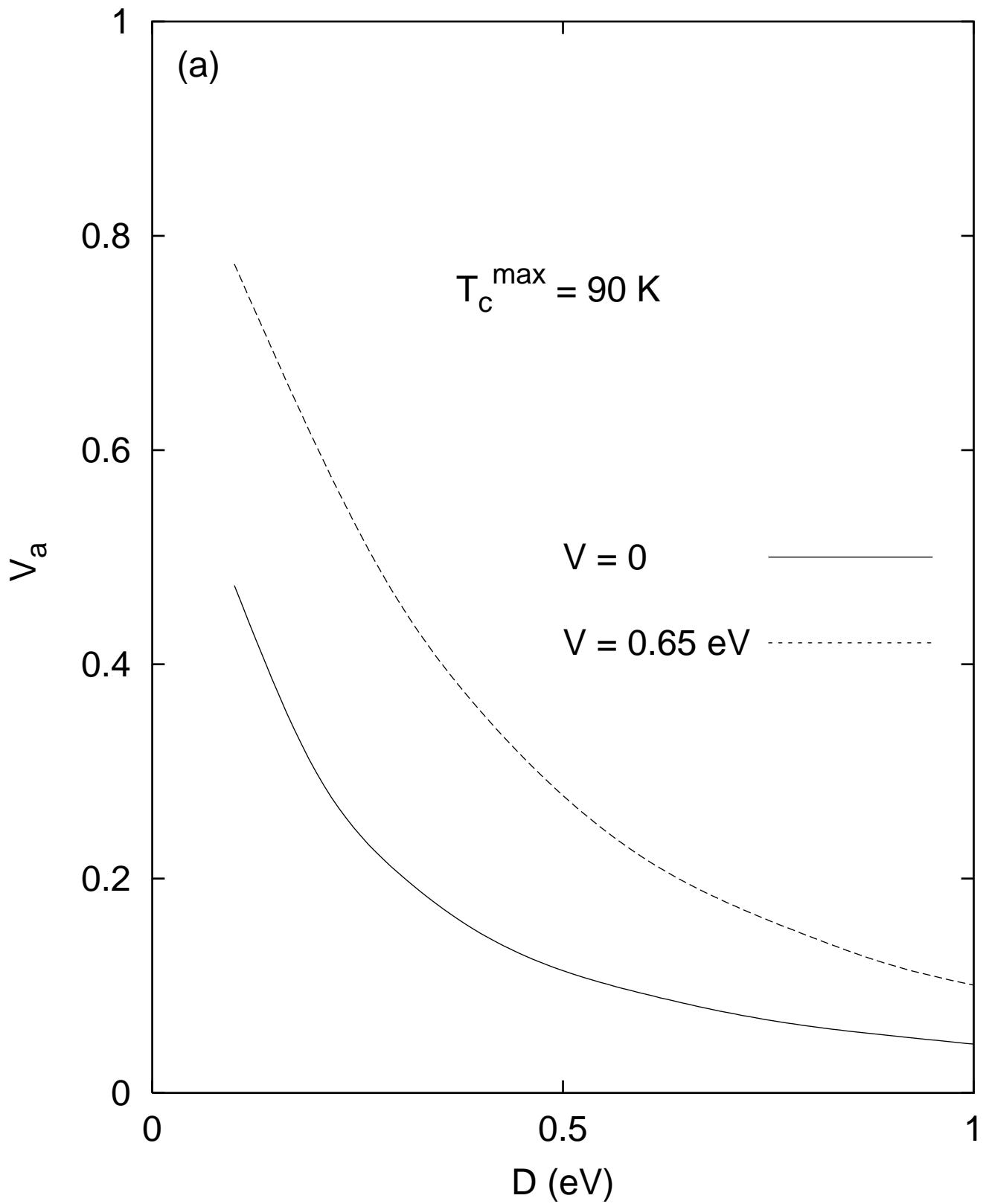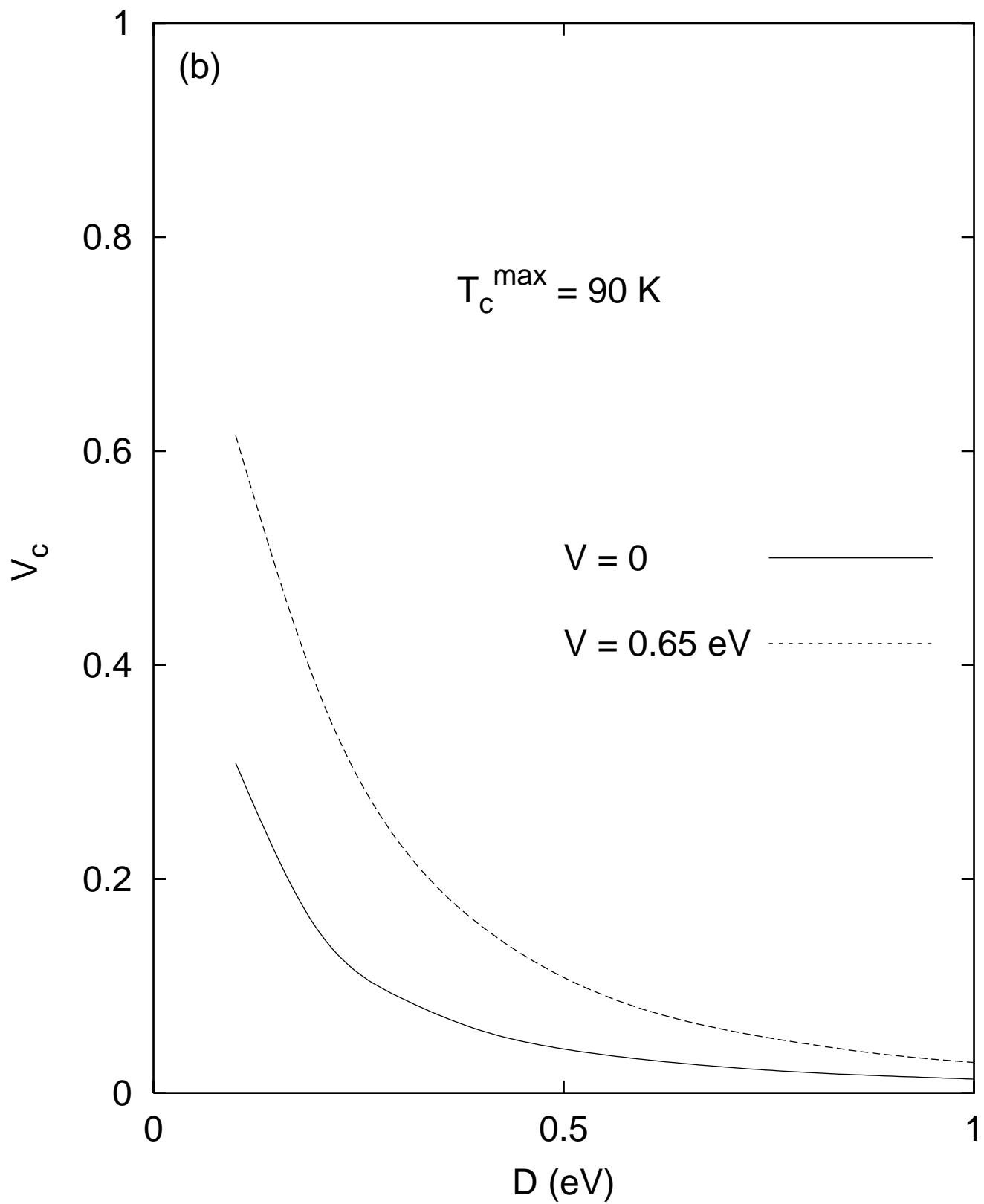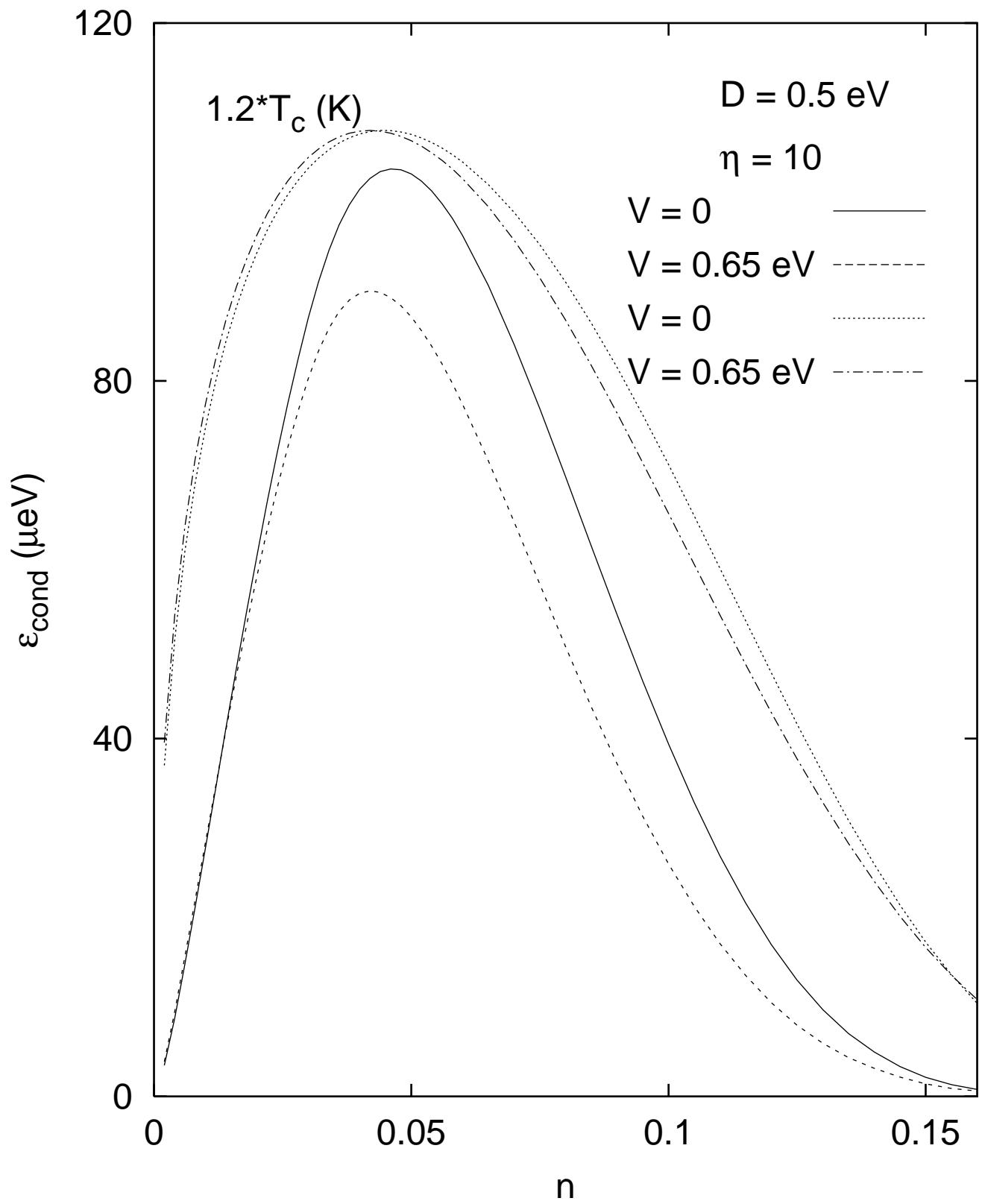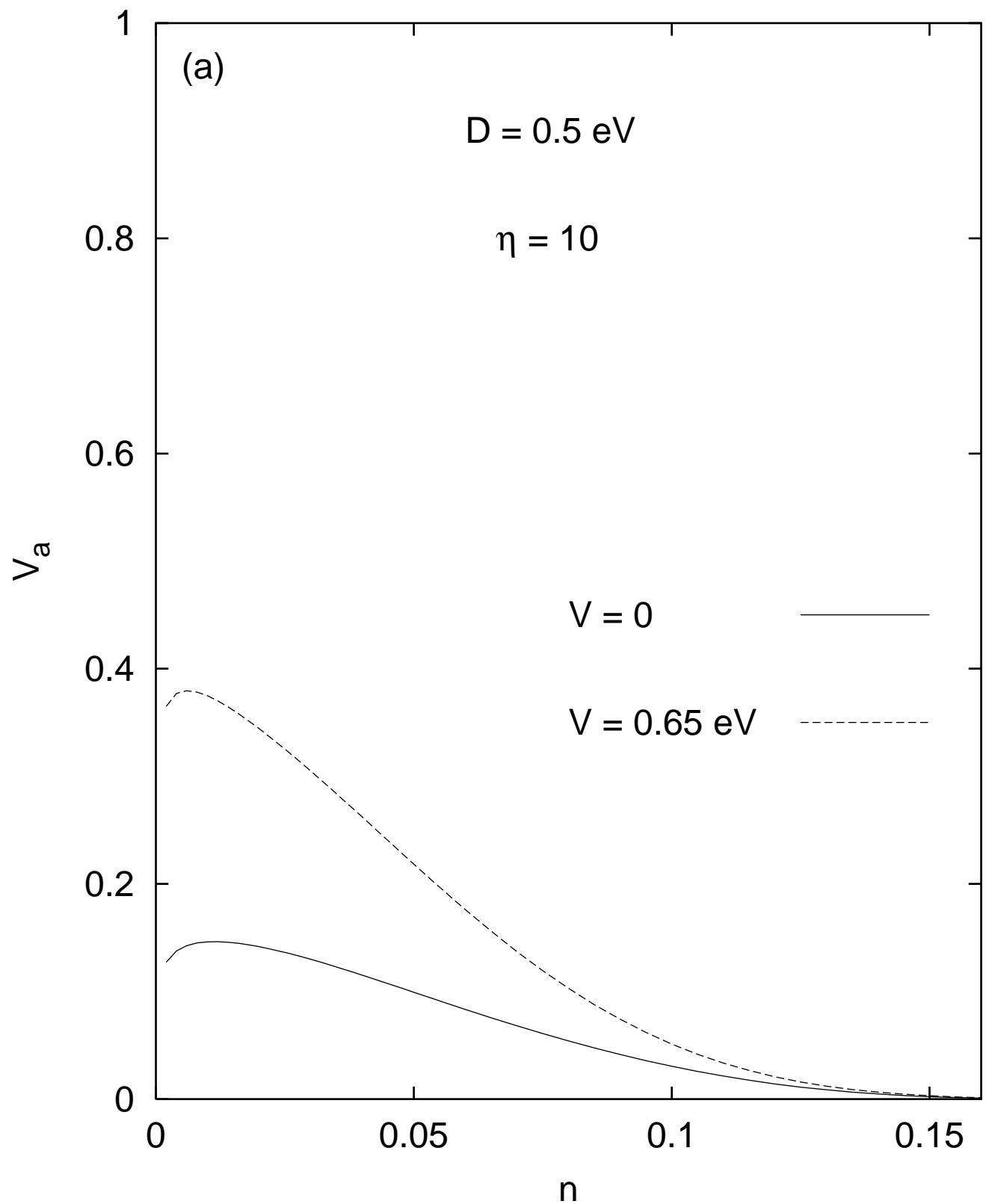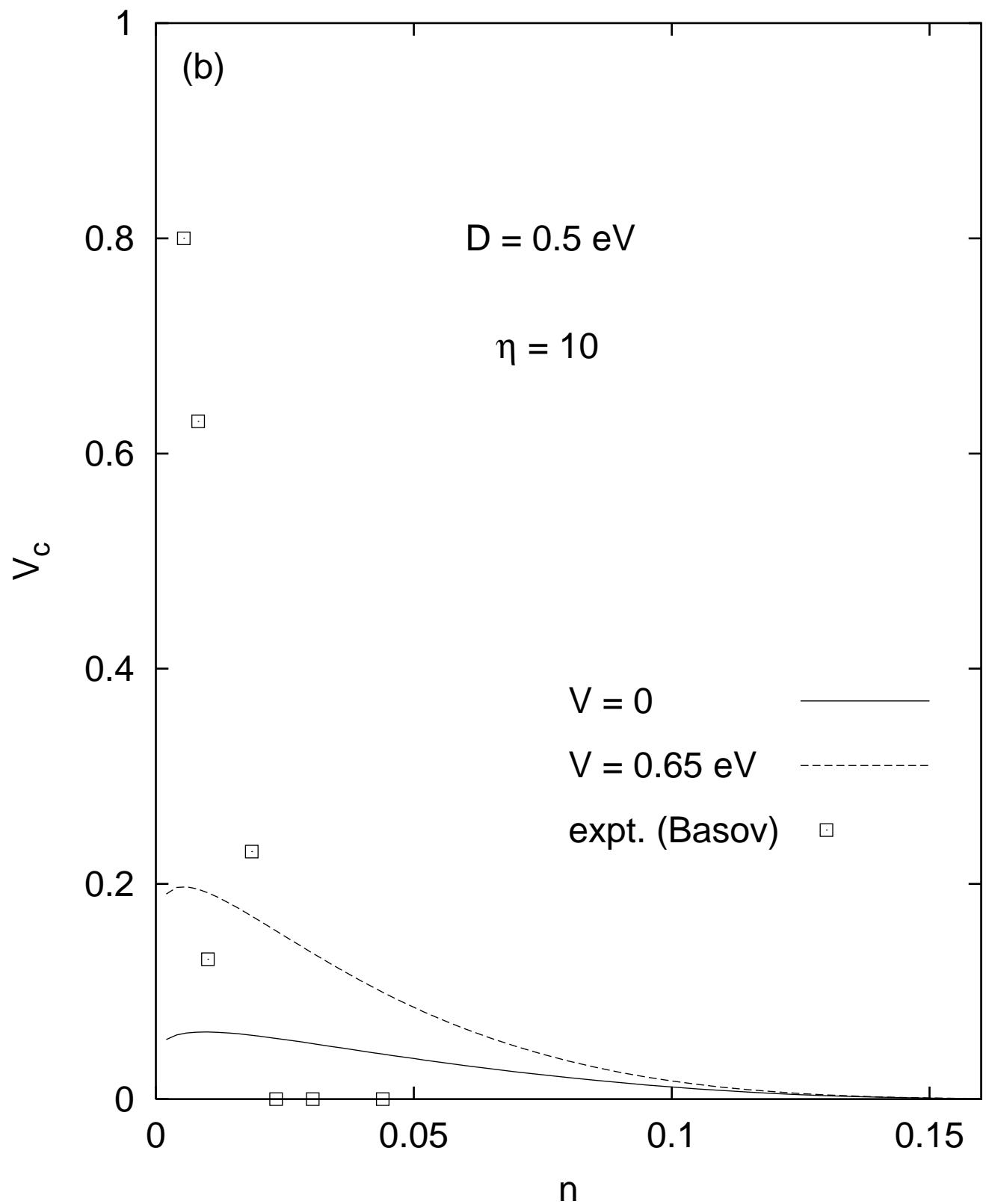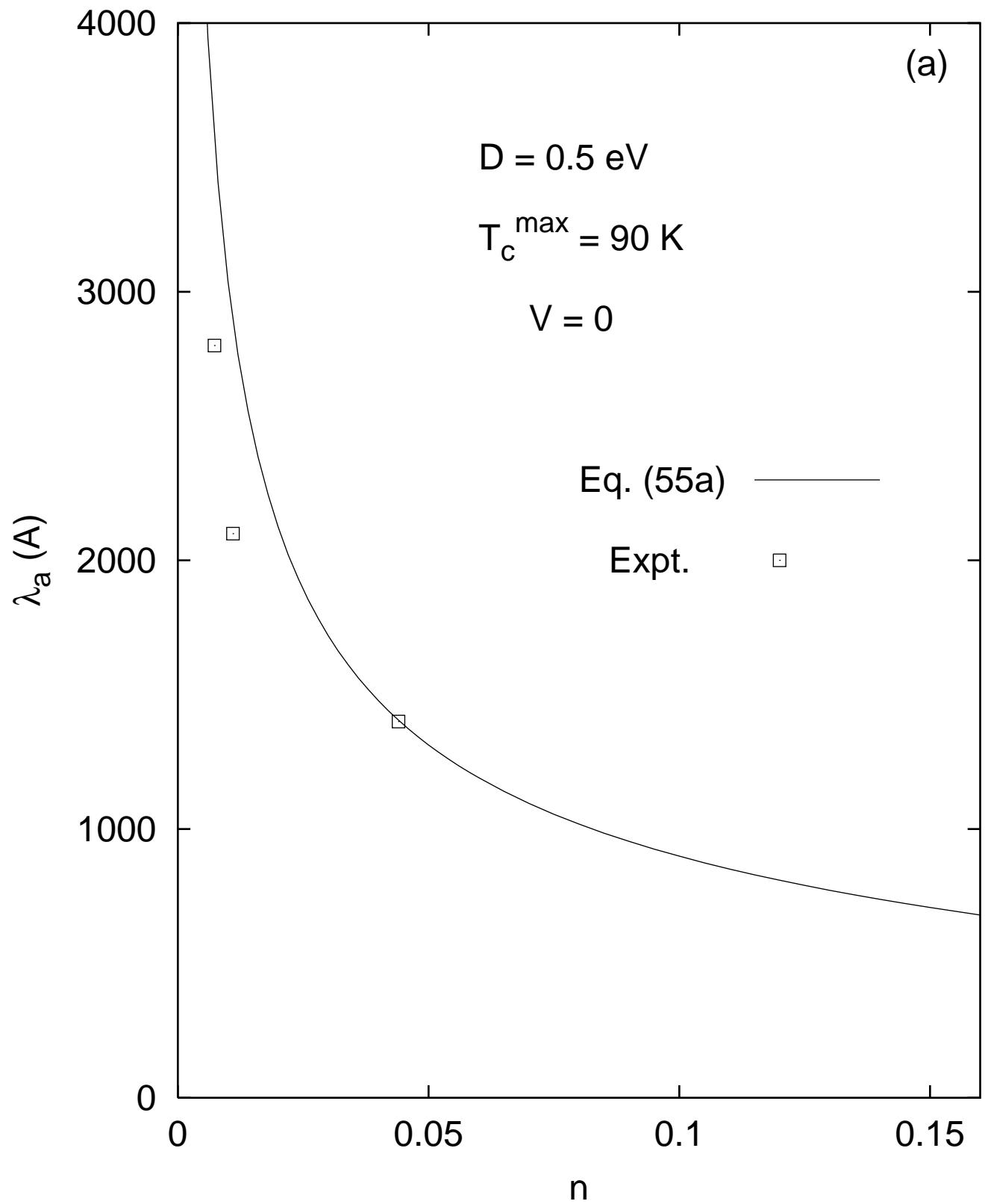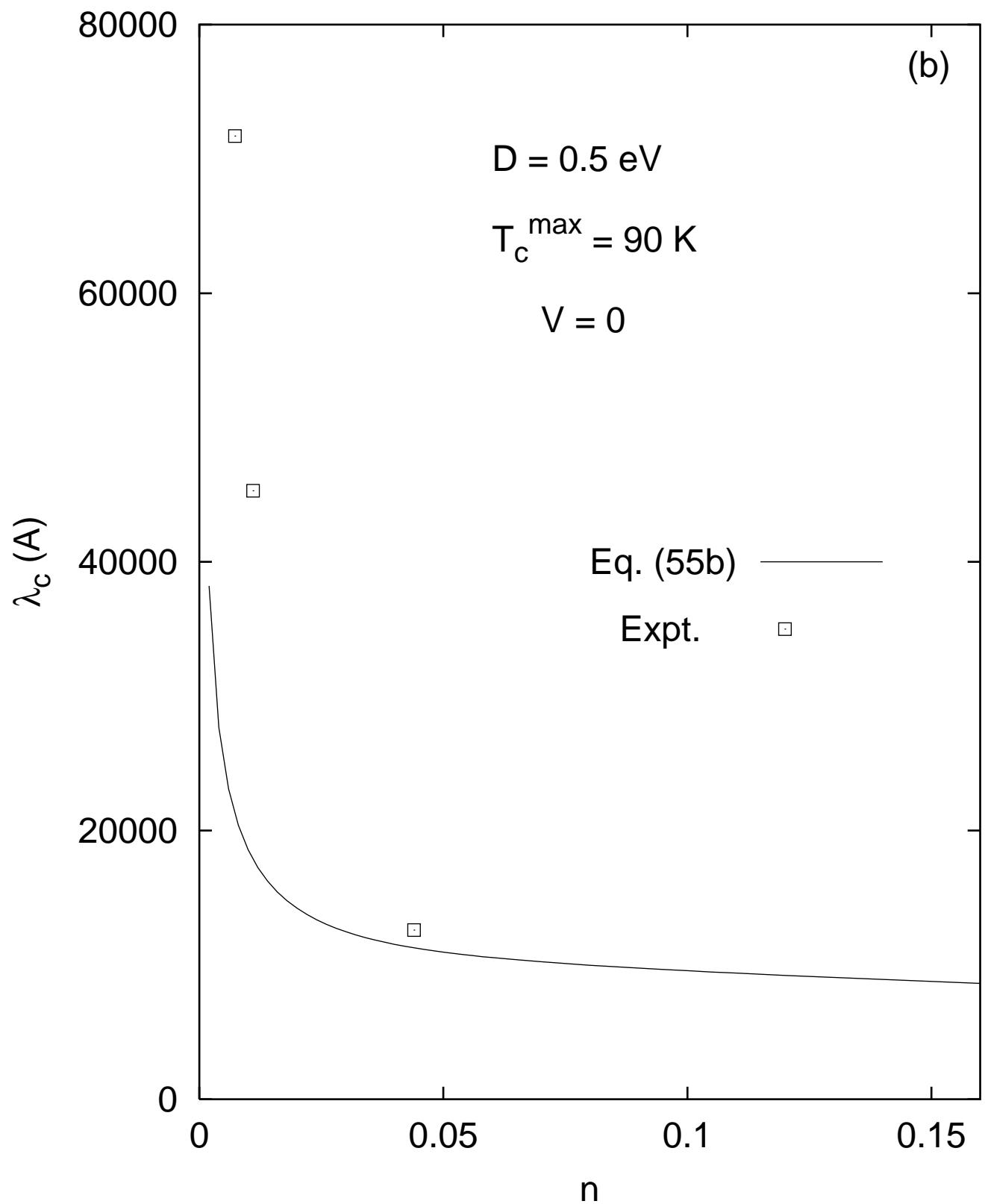
fig21
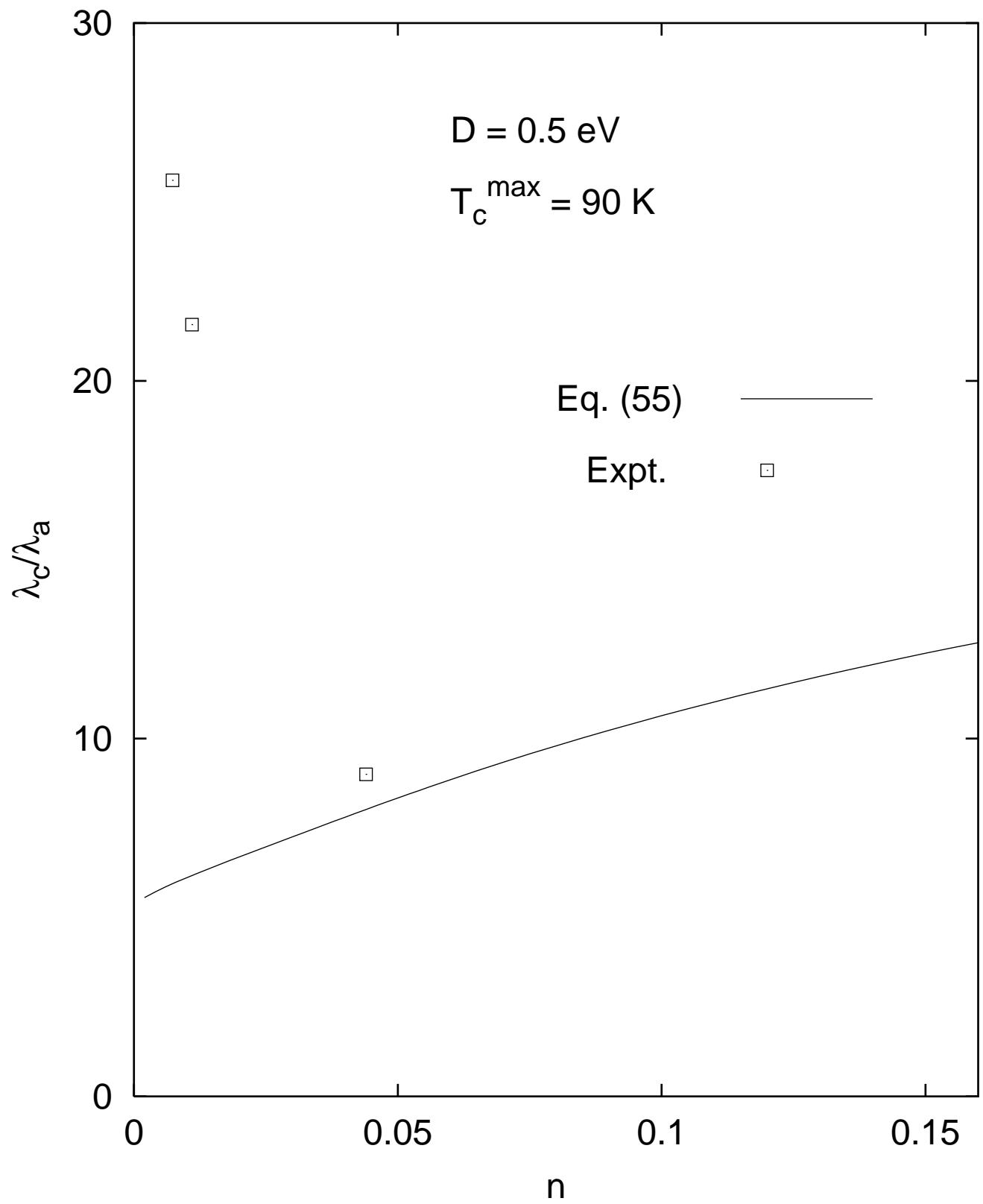
fig22

fig23a

fig23b

fig23c